Chapter 5 (draft copy)

A Closer Look at Regional Curve Standardization of Tree-Ring Records: Justification of the Need, a Warning of Some Pitfalls, and Suggested Improvements in Its Application

Keith R. Briffa and Thomas M. Melvin

Climatic Research Unit, University of East Anglia, Norwich, NR4 7TJ, UK

Abstract

Some background describing the rationale and early development of regional curve standardization (RCS) is provided. It is shown how, in the application of RCS, low-frequency variance is preserved in the mean values of individual series of tree indices, while medium-frequency variance is also preserved in the slopes. Various problems in the use of the RCS approach are highlighted. The first problem arises because RCS detrending removes the average slope (derived from the data for all trees) from each individual tree measurement series. This operation results in a pervasive 'trend-in-signal' bias, which occurs when the underlying growth-forcing signal has variance on timescales that approach or exceed the length of the chronology. Even in a long chronology (i.e., including subfossil data), this effect will bias the start and end of the RCS chronology. Two particular problems associated with the use of RCS on contemporaneously growing trees, which might represent a typical (i.e., modern) sample, are also discussed. The first is the biasing of the RCS curve by the residual climate signal in age-aligned samples and the undesirable subsequent removal of this signal variance in RCS application. The second is the 'differing-contemporaneous-growth-rate' bias that effectively imparts a spurious trend over the span of a modern chronology. The first of these two can be mitigated by the application of 'signal-free' RCS. The second problem is more insidious and can only be overcome by the use of multiple sub-RCS curves, with a concomitant potential loss of some longer-timescale climate variance. Examples of potential biasing problems in the application of RCS are illustrated by reference to several published studies. Further implications and suggested directions for necessary further development of the RCS concept are discussed.

5.1 Introduction

Among those high-resolution environmental proxies that have the potential to express aspects of climate variability with perfect dating fidelity, at annual resolution, tree-ring records remain unique in the way in which they provide information continuously spanning centuries to millennia over vast swathes of the world's extratropical land areas. In general, this information is most accurate in its representation of short-timescale variability; i.e., relative changes from year to year and decade to decade. It is in this high-frequency part of the variance spectrum that chronology confidence can be quantified most easily, and the empirical calibration of tree-ring chronologies, routinely achieved by regression against observed climate variability, can be more accurately facilitated and subjected to rigorous verification through comparison with independent data (Fritts 1976, Section 5.4; Fritts and Guiot 1990; Briffa 1999).

Tree-ring data series, extracted from radial tree-growth measurements, may contain information about external growth influences on multidecadal, centennial, and even longer timescales. The expression of this information in individual series of measurements is, however, obscured by trends associated with changing tree geometry over time. In localized site chronologies and in large regional average chronologies, the expression and reliability of long-timescale variance is affected by the techniques used to 'standardize' the measurements to mitigate non-climate effects and by the manner in which the resulting standardized indices are incorporated within the final chronology. In this discussion, for convenience, we define medium-frequency variability as that representing timescales of decades up to the age of a tree. We define low-frequency variability as that manifested at timescales beyond the age of a tree.

We begin this review by citing a simple example that demonstrates why, where the intention is to recover evidence of long-timescale climate variability in chronologies, it is inappropriate to use common 'data-adaptive' standardization techniques (Cook et al. 1995). We also show how the presence of medium-frequency common tree-growth influences can create distortion in the recovered climate signal, particularly at the ends of chronologies standardized by using flexible curve-fitting techniques.

We provide some background to the history and simple application of what is known today as regional curve standardization (RCS), a standardization approach that has the potential to preserve the evidence of long-timescale forcing of tree growth. We discuss a number of potential biases that arise in the simple application of RCS. We provide some illustrative examples of potential bias issues that have arisen in selected applications of RCS in previous published work. Finally, we suggest some ways in which the potential problems we have highlighted might be addressed in future work.

5.2 Frequency limitation in curve-fitting standardization

We now know that some types of tree-ring standardization are not ideal where there is a specific requirement to compare the growth rates of trees over long periods of time. The fitting of linear or curvilinear functions, or even more flexible forms of low-pass filtering, to series of individual growth measurements and the subsequent removal of variance associated with these trends, results in the inevitable loss of longer-timescale information, even in relatively long measurement series; i.e., the so-called segment length curse (Briffa et al. 1992; Cook et al. 1995).

As an illustration of the loss of low-frequency variance incurred by fitting functions through measured growth parameter series, we show Figure 5.1, based on Figure 1 in Cook et al. (1995). This figure shows the 'standardization' of a pseudo-climate signal comprising the arithmetic sum of three sine waves (with periods of 250, 500, and 1,000 years, each with an amplitude of two units, plotted with their phases synchronized so the curves coincide every 500 years), achieved, in the original work, by subtraction of the values of a straight line fitted through the single composite series. The loss of the original 1,000-year trend in the resulting index series is plain. However, what is also clear is that the higher-frequency variance represented by the sum of the two shorter-period sine waves (dotted line in Fig. 5.1c) has been severely distorted at both ends of the chronology (compare the dotted and solid lines in Fig. 5.1c). This distortion comes about because of the localized influence of the medium-frequency signal variance at the beginning and end of the composite series on the overall fit of the standardizing line. Here the first and last values of the

signal are both zero, while the first and last values of the indices are at their minimum and maximum, respectively. Had this example extended over another 500 years (i.e., 1,500 years), the aggregate signal series would have had zero slope overall. Standardizing with a straight line fitted through the data would not produce any distortion of medium-frequency signal in the index series. This potential end-effect phenomenon, or 'trend distortion,' encountered in data-adaptive approaches to curve fitting in tree-ring standardization is discussed in more detail in Melvin and Briffa (2008). We return to this issue in the context of RCS later.
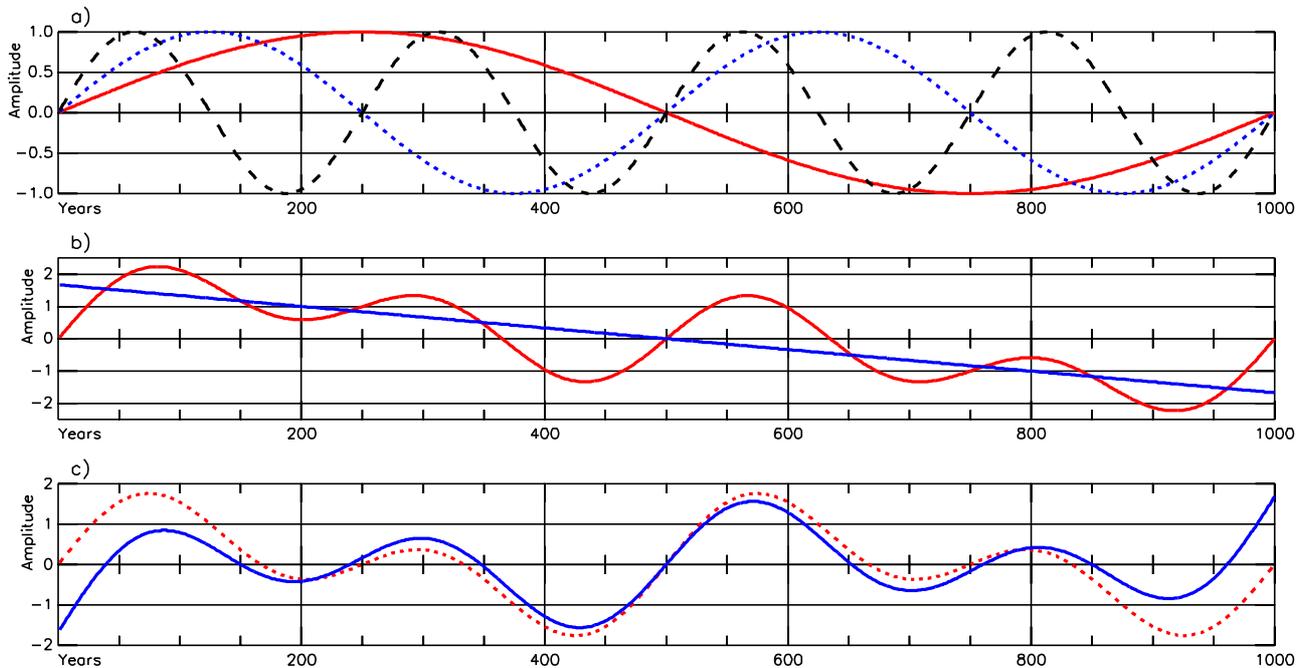
Figure 5.1. An example of the loss of long-timescale variance resulting from simple data-adaptive standardization (in this case, linear detrending), based on the example of Figure 1 in Cook et al. (1995): (a) three sine waves with periods of 1,000, 500, and 250 years; (b) the ideal 'signal' series made as a composite of the three sine waves A linear trend line is shown fitted through these data; (c) indices generated by division of the signal series values by those of the trend line (solid line) and a composite of the original 500- and 250-year sine waves (dashed line), showing the distortion apparent near the ends of the 'chronology.'

5.3   Background and description of regional curve standardization

The limitations in preserving evidence of long-timescale climate change in chronologies, led to the reintroduction of what is now generally known as regional curve standardization. This approach scales ring measurements by comparison against an expectation of growth for the appropriate age of ring for that type of tree in that region (Briffa et al. 1992a). The tree-ring measurements acquired from multiple trees in one area are aligned by ring age (years from pith), and the arithmetic means of ring width for each ring age are calculated. The curve created from the mean of ring width for each ring age is smoothed by using a suitable mathematical smoothing function (Briffa et al. 1992; Esper et al. 2003; Melvin et al. 2007) to create smoothly varying RCS curve values for each ring age. In a simple application of RCS, each ring measurement is divided by the RCS curve value for the appropriate ring age to create a tree index (note in all cases subsequently discussed here, indices are created by division of the expected into measured values). Chronology indices are created as the

arithmetic mean of tree indices for each calendar year. The value of the expected growth curve is, therefore, empirically derived as the average value, for that tree-growth parameter for the specific age of ring, based on the available sample of trees from that site or region. The reordering of the data, from calendar to relative life span age, is intended to remove the effect of climate variability on expected ring growth. In the reordered alignment of the data, this climate-related variance is assumed to be distributed randomly and expected to cancel out when the age-aligned data are averaged to form the RCS curve.

In standardization applications where the means of index series are constrained to be equal (e.g., approximately 1.0), a chronology formed by averaging these data is not capable of representing variance on timescales longer than the lengths of constituent series. The means of series of tree indices are not constrained in RCS, and it is because the means of index series from different trees can vary through time, that the chronology constructed from them can exhibit long-timescale variance at periods up to the length of the chronology or beyond (Briffa et al. 1992; Cook et al. 1995; Briffa et al. 1996).

The use of the curve formed by calculating mean ring width of radial measurements ordered by cambial age has a long history in forestry and dendroclimatic studies, and an earlier awareness of some of the problems associated with it can be recognized. In seeking to study past climate changes in California, Huntington (1914) used a curve of growth rate plotted against ring age, which included a correction for longevity because he recognized that older trees tended to grow more slowly, even when young, compared to others. In a study of the relationship between tree growth and climate in Sweden, Erlandsson (1936) calculated growth rate curves for specific age classes of trees at various locations and applied a correction factor to enable comparison of different age classes. Mitchell (1967) showed that the shape of the mean curve by ring age varied between species and for the same species in different geographical locations. Becker (1989) used trees from generally even-aged, living stands but selected a large number of stands with as wide a range of stand ages as possible in order to eliminate the effect of 'trends according to calendar years.' Dupouey et al. (1992) developed a mean growth by age curve to model and remove the age trend while retaining long-timescale variance. Briffa et al. (1992a, 1996) introduced the term 'regional curve standardization' to describe the method in the specific context of attempting to recover long-timescale climate trends but used large numbers of subfossil trees, hoping to eliminate the problem of modern climate biasing the parameters of the RCS curve.

Nicolussi et al. (1995) examined how tree-growth rates change when they are quantified for a specific ring age class through time and discussed problems associated with the interpretation of these changes. Badeau et al. (1996) examined potential sources of bias in the use of regionally based age curves. Esper et al. (2002) used two different RCS curves to standardize tree measurements from a wide range of sites being analyzed together, and Esper et al. (2003) also examined other aspects of RCS implementation. Helama et al. (2005a) examined the effect of forest density on the shape of the RCS curve.

Since its recent reintroduction for dendroclimatic studies, there has been a resurgence in the application of RCS, and it has been adopted and sometimes adapted in dendroclimatic studies intended to capture long-timescale climate variance (e.g., Rathgeber et al. 1999a; Cook et al. 2000; Grudd et al. 2002; Helama et al. 2002; Melvin 2004; Naurzbaev et al. 2004; Büntgen et al. 2005; D'Arrigo et al. 2005; Linderholm and Gunnarson 2005; Luckman and Wilson 2005; Wilson et al. 2005)

5.4   Potential biases in RCS

Previous discussions of the recent application of RCS make it clear that the advantage offered by this approach, in terms of its potential to represent long-timescale variability in chronologies, must be weighed against the likelihood of large uncertainty associated with this information. Fritts (1976, p. 280) pointed out problems with the use of RCS when he stated, '… all individuals of a species rarely attain optimum growth at the same age, and individual trees differ in their growth rates because of differences in soil factors, competition, microclimate, and other factors governing the productivity of a site.'

In practice, the simple application of RCS as described above makes sweeping assumptions about the validity of using a single, empirically derived curve to represent 'expected' radial tree growth as a function of tree age under constant climate conditions, and that this simple curve is an appropriate benchmark for scaling measured ring widths throughout the entire time span of a chronology. It is assumed that the mean of tree-growth deviations from this expectation, as observed in multiple tree samples at any one time, represents the net tree-growth response to variations in climate forcing alone. It is assumed that the form of the RCS curve is unbiased by the presence of residual climate variability in the stacked average of cambial-age-aligned samples, and that through time the growth of sample trees is not biased by some factors other than climate that would lead to a misinterpretation of the RCS chronology variability. In practice, these assumptions are unlikely to be entirely valid. The purpose of this review is to draw attention to several examples of how different potential sources of bias can affect RCS chronologies.

5.4.1   'Trend-in-signal' bias

The first distortion of underlying common forcing signal occurs in RCS when that signal has variance on timescales that approach or are longer than the length of the chronology. As a hypothetical example, let us say that the climate affecting tree growth has a trend over 600 years (Fig. 5.2a; actually, this series represents a negative trend with added white noise smoothed with a 10-year spline to represent short-timescale climate forcing superimposed on the long-term forcing trend). This signal series can be subdivided into five 200-year-long series, each overlapping by 100 years, to represent a set of pseudo-tree-ring measurement series (Fig. 5.2b). Aligning these series by ring age (Fig. 5.2c), averaging and smoothing, produces the RCS curve (shown in Fig. 5.2d). This RCS curve displays the mean slope of all sample series. As they all contain the underlying long-term forcing signal, the RCS curve must do likewise. Each sample measurement series is then indexed by dividing by the appropriate age value of the RCS curve. Each of the resulting standardized series (Fig. 5.2e) has no substantial overall trend (i.e., the mean series of the age-aligned index series has zero trend).

When the index series are realigned by calendar year, each series systematically underestimates the magnitude of the ideal forcing in its early section and overestimates the signal later, a potential medium-frequency bias. In the average chronology (Fig. 5.2f), the original overall signal trend is captured by the differences in the means of the index series. In our simplified example, the bias in the trends of individual index series cancel to some extent by virtue of the compensating biases in overlaps between early sections of some index series and late sections of others. In situations where there is a good overlap in many series, this potential bias could be averaged out. However, this cannot happen at the start and end of the chronology. In the case of a long-term declining signal, the

chronology will, respectively, under- and overestimate the ideal chronology at the beginning and end. With a long-term positive forcing trend, the signs of the biases will be reversed.
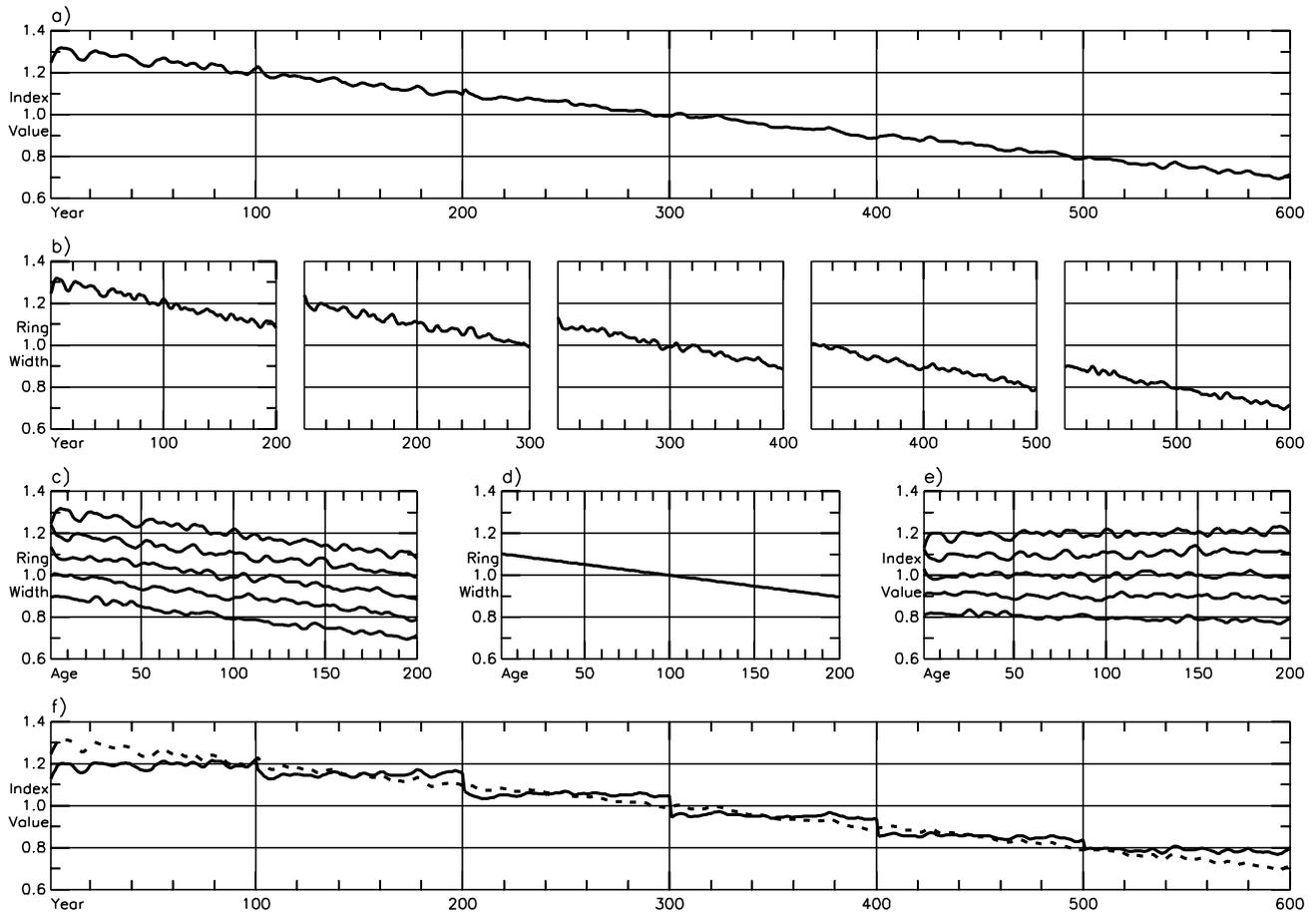
Figure 5.2. A schematic representation of how the simple regional curve standardization (RCS) recovers long-timescale trend from the mean values of index series but with potential distortions within, and particularly at the ends, of the chronology: (a) an idealized chronology signal composed of an overall negative slope with superimposed medium-frequency variance; (b) five overlapping 200-year-long series representing simulated measurements; (c) the five series aligned by ring age; (d) the smoothed RCS curve generated by averaging these series; (e) the series of indices generated through division by the RCS curve; (f) the averages of these indices that make up the resultant chronology (solid line), which is shown superimposed on the ideal chronology (dashed line).

Figure 5.3 illustrates a somewhat more realistic example of this problem than that shown in Figure 5.2. The underlying forcing signal that is used here is similar to that used in Figure 5.1, but rescaled to resemble ring measurements (white noise with mean of 1.0 and range ±5% was smoothed with a 10-year low-pass filter added to the three sine waves, each of which has an amplitude of 0.34). This aggregated sine wave signal series was sub-sampled to produce forty-one 334-year pseudo-measurement series. Their start dates are evenly distributed between year 1 and year 668, providing the potential for a 1,002-year chronology with a maximum replication of 20 series (see shaded area in Fig. 5.3d). Figure 5.3a shows five of the sample series. Figure 5.3b shows the average of age-aligned measurements of all 41 series, and Figure 5.3c shows the same five example series from Figure 5.3a, after standardization with the average RCS curve. Figure 5.3d shows how the medium-

and long-term trends in the underlying forcing are relatively well represented in the RCS chronology. The loss of long-timescale signal apparent in Figure 5.1c does not occur in Figure 5.3d. However, the systematic under- and overrepresentation of the aggregate signal (in years 1 to 300 and 700 to 1002, respectively) results from the trend-in-signal bias, similar to the biased representation of the medium-frequency signal shown in Figure 5.1c. The trend-in-signal bias is generally manifested as an end-effect problem in both RCS and curve-fitting standardization. However (because trend distortion is the result of slope removal), while in the latter case the entire slope of an individual-tree measurement series is removed, in the case of RCS, only the mean slope over the whole length of the chronology is removed (i.e., implying a much smaller-scale problem of overall trend distortion in RCS).

Note that by applying the recently advocated 'signal-free' method of standardization (see Appendix), this problem may largely be mitigated in the RCS. For example, when applied to the data in Figure 5.3, this approach is able to capture all of the long-timescale variance and it does so without producing this end-effect bias. For these equal-length, artificial series, the 'ideal' chronology signal is recovered without distortion as shown by the blue curve of Figure 5.3c. However, it is important to stress that in this highly artificial example, all of the index series have the correct means and amplitude of variance, perfectly matching the hypothesized signal. In a 'real-world' situation, random variation in growth rates of trees would prevent such a perfect result.
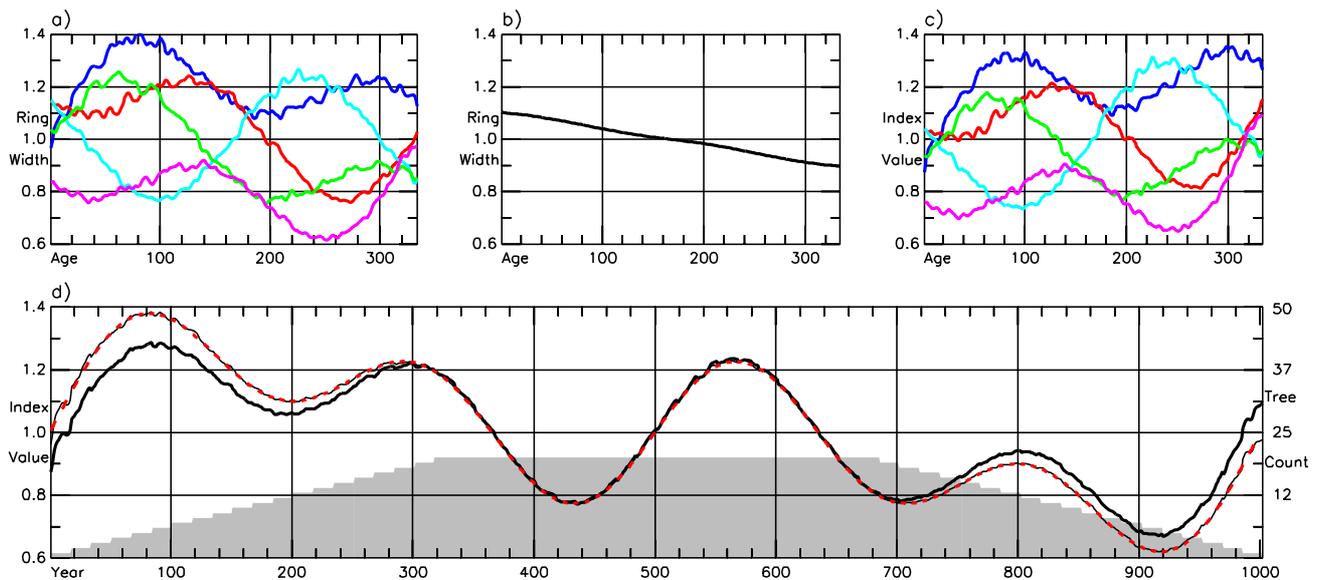
Figure 5.3. An example of the use of regional curve standardization (RCS) where the 'signal' is the same composite of the three sine waves shown in Figure 5.1a: (a) five sample series; (b) smoothed, mean RCS curve of all 41 series; (c) indices of the five example series created by division with the RCS curve; (d) the ideal chronology (dashed line; as in Fig. 5.1b), the RCS chronology (thick line) with 'trend-in-signal' bias apparent at the start and end of the chronology. Sample counts are shown by grey shading. A substantially undistorted recovery of the 1,000-year trend (thin line), and the variance associated with the shorter-period sine waves is achieved in using the 'signal-free' approach discussed in the Appendix.

5.4.2   'Differing-contemporaneous-growth-rate' bias

The second potential end-effect bias arises because, even within one region, there is often a variation in the growth rates of contemporaneously growing trees. The problem that a single RCS curve may not be relevant for trees with widely varying growth rates has been widely recognized (e.g., Erlandsson 1936; Nicolussi et al. 1995; Briffa et al. 1996; Rathgeber et al. 1999a; Esper et al. 2002). In a restricted geographical range where trees might be expected to experience the same regional climate, localized elevation or aspect differences can lead to variations in the climates of specific tree locations. Even where trees do experience the same common history of climate forcing during their lifetime, invariably, some trees will exhibit greater or less radial growth than others because they are influenced by non-climatic factors such as differences in soil quality or competition for light or other resources. A simple RCS approach uses a single (average) model of expected tree growth (e.g., radial ring increment or maximum latewood density) as a function of tree age, applied to all trees in one region. If trees are drawn from a wide region or one with diverse ecological conditions, differences in growth rate in contemporaneously growing trees is virtually inevitable. Within such a sample, the slope of a single average RCS curve will be systematically too shallow for relatively fast-growing trees and too steep for relatively slow-growing trees (Fig. 5.4).

This mismatch is most apparent for the indices that are produced from earlier years of the tree lifetime, as the sub-RCS curves for fast- and slow-grown trees (Fig. 5.4b) often tend to a common value in old age and the corresponding index series, produced as quotients from the overall mean RCS curve, display a negative trend for the early years of a fast-grown tree and a positive trend in the early years of a relatively slow-grown tree (Fig. 5.4c). In an RCS chronology, if in one period fast-grown trees outnumber slow-growing trees (or vice versa), artificial medium-frequency trends (i.e., of non-climate origin) might result. It is at the recent end of a chronology that the influence of downsloping indices, derived from fast-growing trees, may not, in general, be balanced by the upsloping index series from slower-growing trees. The result, even under constant climate conditions, is an overall negative bias, seen in the final century or most recent decades of the chronology.
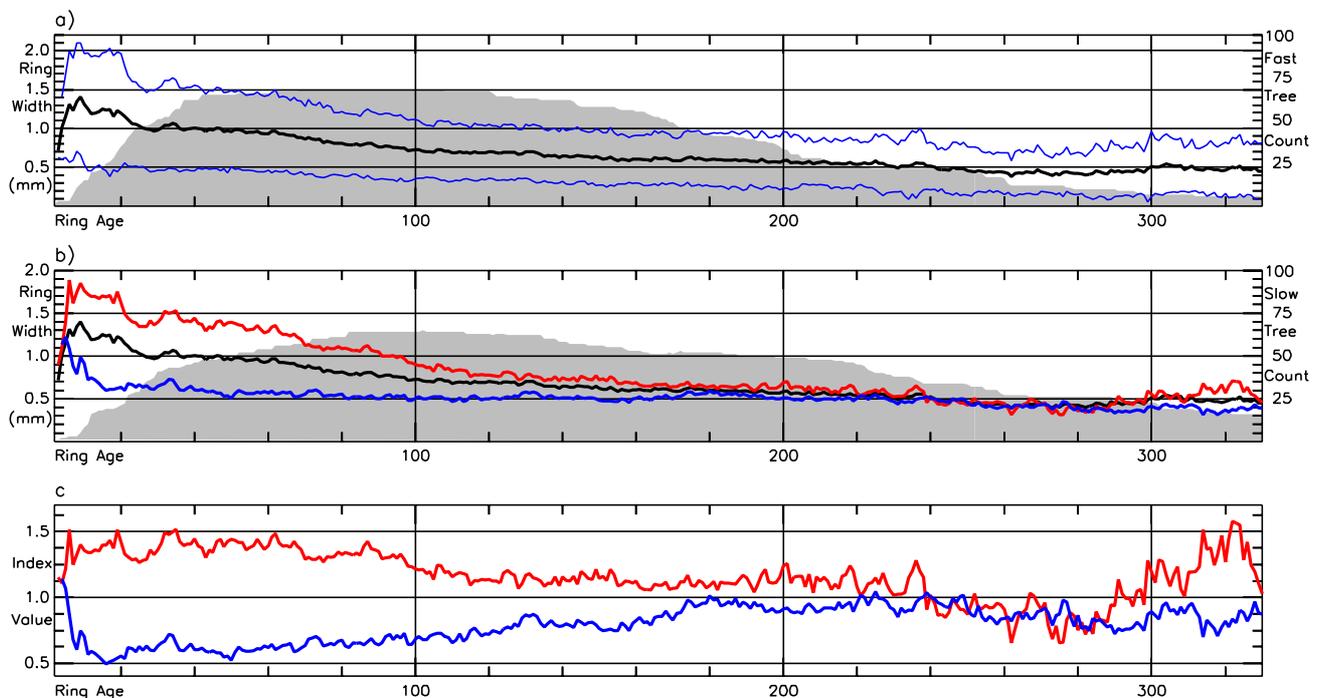
Figure 5.4. Based on 207 measurement series, for which pith-offset estimates are available (Kershaw 2007), from the AD portion of the Swedish Torneträsk chronology (Grudd 2002): (a) curve of mean ring width by ring age, bracketed by thin lines showing the plus and minus one standard deviation limits of the mean values; (b) separate curves of mean ring width by ring age for all trees (middle line - as in 5.4a), the fastest-growing third of trees (upper line), and the slowest-growing third of trees (lower line); (c) mean ring width indices (produced by dividing the measurements by the appropriate age values on the overall-mean regional curve standardization curve), plotted by ring age for the fastest-growing third of trees (upper line) and the slowest-growing third of trees (lower line). The gray shading in (a) and (b) shows sample replication for the fastest- and slowest-growing trees, respectively.

5.4.3 'Modern-sample' bias

The next bias we discuss has been referred to by Melvin (2004, Section 5.4) as 'modern-sample bias.' We consider this of sufficient importance to identify it as a specific potential bias in its own right, but it arises as a consequence of the previously discussed bias (i.e., because of different growth rates in contemporaneous trees) and because of variations in the longevity of trees, allied to common tree sampling practice.

A naturally grown, uneven-aged forest (even if growing in an unchanging climate) will contain trees of differing ages that have roughly the same diameter. The widths of rings of a specific age from trees of the same diameter must be smaller for the older trees than for the younger trees. A plot of mean ring width for a specific ring age plotted by calendar year for a specific sampling diameter range (i.e., only for trees of a similar diameter when cored) will display a steady increase over time, independent of any common climate signal. If samples are taken only from trees alive on the sampling date, then the mean growth rate by year (as the average of each diameter class for any specific age range, which all slope upwards) must also slope upwards.

5.4.3.1   Relationship between growth rate and longevity

This bias arises if there is a relationship between average tree growth rate and tree longevity and generally applies only to trees with full circumferential growth. If we assume that the probability of tree mortality is related to tree size—i.e., large trees have a high risk of mortality—then as trees approach the largest size for a given site, they are much more likely to be killed, perhaps because of some extreme climate event. Hence, the likelihood that some random extreme event will kill a tree is higher while it is in the 'near maximum' size category. Rapidly growing trees are more likely to approach or reach the maximum size than are slower growing trees because the former need only spend a shorter time in the 'high-risk' (i.e., approaching large) size category (Melvin 2004, Section 5.4). To grow old, a tree must grow slowly and so remain for some considerable time, safely below the maximum size by some margin.

This, of course, is a great simplification of likely tree mortality influences. It takes no account of the competition dynamics of trees growing within forest stands; i.e., self-thinning processes (Dewar 1993). Nevertheless, there is some observational evidence, particularly when competition pressures are not strong, that to become old a tree might grow slowly (Huntington 1913). Figure 5.5 is an attempt to demonstrate this concept using subfossil pine ring width data from northern Fennoscandia (Eronen et al. 2002; Grudd et al. 2002). These wood samples provide data that span the last 7,500 years, but here we have excluded any data from trees that were alive after 1724. This choice precludes any human sampling influence on the life span of trees. The retained data were used to produce a single RCS curve. The measurement data for each tree sample were then summed to

provide an estimated diameter, and this diameter was compared to the mean regional diameter calculated from the appropriate age point of the RCS curve to give a relative growth rate (i.e., the ratio of tree diameter at its final year to the RCS curve diameter at that year). In this way, all the individual tree measurement series were grouped into eight relative growth classes and a sub-RCS curve was constructed for each relative class. The mean growth rate (millimeters per year) by age for these eight RCS curves is shown in Figure 5.5a, and the decay in mean growth rate is due to the reduction of ring width with age. A tendency for higher growth-rate classes to have shorter life spans can be discerned. Plotting the mean growth rates of individual samples by sample age (i.e., final tree diameter divided by final age) again reveals a tendency for slowly growing trees to live longer (Fig. 5.5b). The oldest trees have mean growth rates far lower than the reduction explained by the expected decrease of ring width with age shown in the curves of Figure 5.5a. This occurs despite the fact that many subfossil tree samples lose outer rings because of erosion or degradation of the relatively soft sapwood.
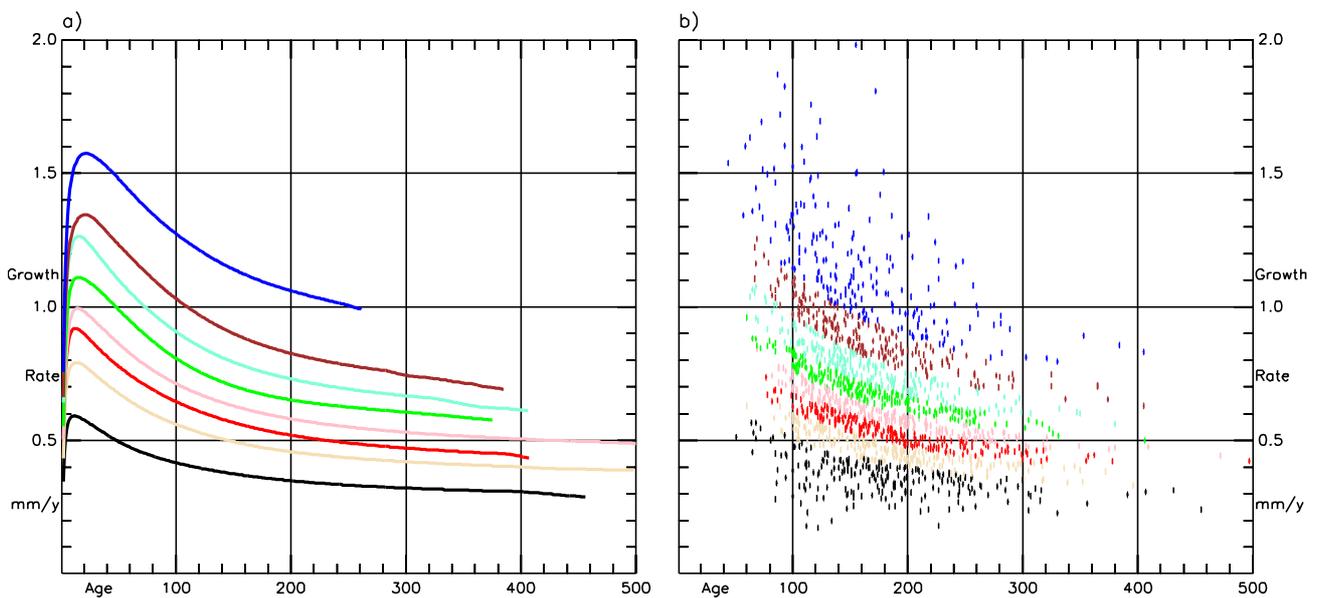
Figure 5.5. Based on 1724 subfossil trees from Torneträsk (Grudd 2002) and Finnish Lapland (Eronen 2002) from the period circa 5400 BC to AD 1724; i.e., excluding trees that were alive after 1724 to avoid any anthropogenic factors and sampling bias: (a) all trees sorted by growth rate relative to a single regional curve standardization (RCS) curve, into eight separate RCS curves; (b) a scatter plot of mean growth rate for each tree plotted against final tree age. Scatter plot points are shaded to match their growth rate curve of (a). This figure illustrates the tendency for longevity to be inversely proportional to tree vigor.

5.4.3.2   Growth rate/longevity association distorts RCS curves
Figure 5.6 illustrates a very simplified example of one distortion that occurs where a sample of even-sized (radius 26.4 cm) trees of varying age might be cored (Fig. 5.6a). Here there is an assumed constant climate forcing (horizontal dashed line of Fig. 5.6b) and the younger trees have progressively larger growth rates. The mean RCS curve is horizontal up until 240 years (the age of the youngest tree) but gets progressively lower as the lower growth rates of the older trees dominate. Thus this is a distortion of the RCS curve caused by older trees having lower growth rates. Hence individual index series aligned by calendar age then exhibit positive trends after 240 years (Fig.

5.6c), and the calendar-aligned averaged values (Fig. 5.6d) display an initial (stepped) increasing trend for the first 160 years of the mean chronology due to the oldest trees having slower growth rates, and a late increasing trend after 240 years because of distortion of the RCS curve, despite the fact that the underlying forcing signal is constant. The constant mean growth rate is not realistic, but the bias shown will apply similarly to curvilinear declining ring series.
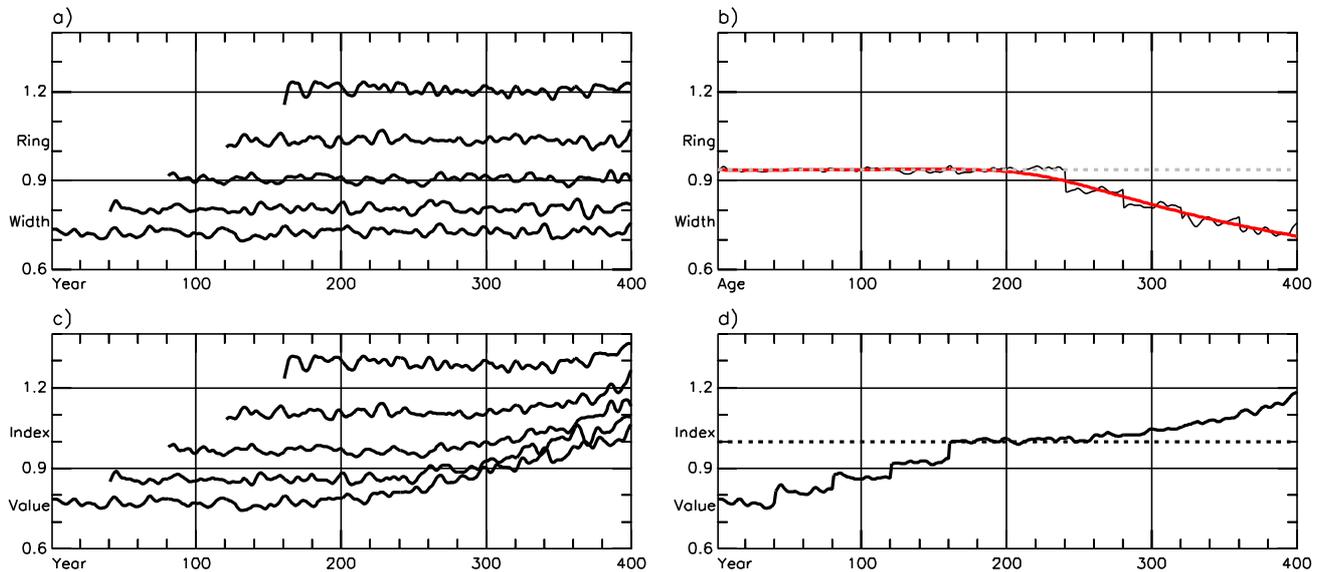
Figure 5.6. A simple hypothetical example of the distortions to a common underlying forcing signal when a chronology is constructed by using regional curve standardization (RCS) applied to an uneven-aged group of similar-sized trees. (a) The measurements from five trees of unequal length and of the same final diameter (26.4 cm), each containing the same trend in growth superimposed on the differing overall average growth. When aligned by ring age, the average RCS curve (b), instead of displaying the expected linear growth trend (dotted line) is distorted, showing narrower expected ring width for older trees. (c) Series of indices created through division of the simulated measurements by the RCS curve values, where all but the shortest series are distorted. (d) The chronology created by averaging the index series and the desired low-frequency signal (dotted line).

In order to demonstrate modern-sample bias, it is necessary to use series of tree indices that have no common climate signal and no common age-related growth trend. Here, 1724 trees from both Torneträsk (Grudd et al. 2002) and Finnish Lapland (Eronen et al. 2002) from the several-millennia period 5400 BCE to AD 1724 are used. Trees that were alive after 1724 are not included so as to avoid any anthropogenic factors or sample bias arising from the coring of living trees. The measurement data are all realigned so that their final growth years correspond (i.e., they are 'end-aligned' and the end year is nominally set to zero). The mean ring width of the subset of all 40- to 60-year-old rings from trees with a final radius between 12 and 14 cm (ring counts shown as gray shading) are plotted by nominal year for Figure 5.7a. In order to reach the 12–14 cm final diameter class, the 40- to 60-year-old rings must be larger for the younger trees than in the older trees and this curve of mean ring width takes on a positive slope. Provided that there is some maximum size limit to tree growth, the sum of data for any, and hence all, size classes will also produce an upwardly sloping common signal. This bias occurs in the absence of any common climate signal, and is a result of random distribution of tree growth rates and the fact that sampling takes place at a specific point in time.

Figure 5.7b shows the yearly means of all RCS indices (based on a single RCS curve) after alignment by their final growth year (year zero). Even though these trees grew at various times over a 7,000-year period, and should not, therefore, contain any common external growth-forcing signal when in this alignment, there is still evidence of a residual bias, represented by a general positive slope as tree counts increase followed by a slight decline in the final period, when tree counts remain constant. This decline is likely the result of indices of 'fast-growing' trees, with their typical negative slope (cf. Fig. 5.4), dominating over the weaker positive trend from 'slow-growing' trees.

This result demonstrates the strong likelihood of sampling bias implicit in analyses of ring width, density, or basal area increments, where the data are stratified within discrete age classes (e.g., Briffa et al. 1992; Nicolussi et al. 1995). Age band decomposition (ABD) as proposed by Briffa et al. (2001), although originally envisaged as a means of circumventing the need to define a statistical model of expected growth as a function of tree age, is in effect similar to applying RCS. This conclusion follows because the mean value for each age band, when plotted as a function of ring age, will form a stepped version of the RCS curve. In ABD, the mean value of the time series for each age band is subtracted from each average yearly value for that band, and these differences are divided by the standard deviation of the band time series to transform the data into normalized series. These series are then summed across all (or selected) age bands to form an ABD chronology. When this method is applied in this way to the data for a single species and location (e.g., see Briffa et al. 2001), it is similar to applying the RCS at a site level to a set of living-tree core samples. The results may, therefore, be affected by a modern-sample bias, bearing in mind the common practice of sampling dominant or codominant trees (Schweingruber and Briffa 1996).
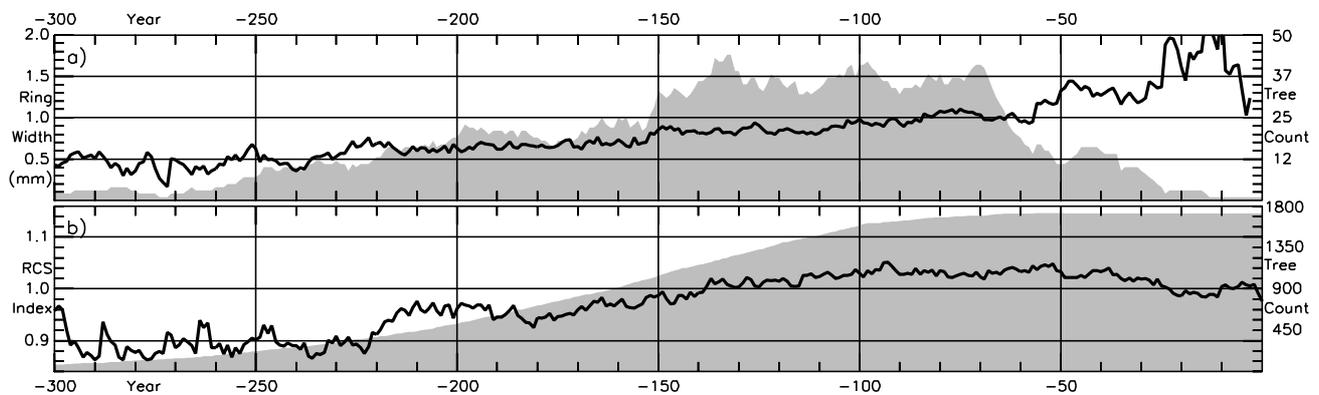
Figure 5.7. Based on the same subfossil tree-ring dataset used in Figure 5.5, but here with all individual series aligned on the final ring of each series (year zero): (a) the mean ring width of the subset of all 40- to 60-year-old rings from trees with a final radius between 12 and 14 cm; (b) indices, created using regional curve standardization (RCS), aligned according to their final year of growth (year zero) and averaged to form an 'end-aligned' chronology. Ring counts for each year are shown by the gray shading.

Where this sampling bias exists, it is difficult to gauge the extent to which it amplifies or obscures the accompanying influence of climate variability. Note that in Figure 5.7b, the range of the bias is only 0.14 units, likely considerably less than the range for typical chronology variances, for

example, as is shown in Figure 3 of Becker (1989) or in Figure S4b of Esper et al. (2007), where chronologies display similar shapes (in their time variance) to that of the bias in Figure 5.7b. Figure 5.8 is a dramatic example of how the selection of samples, based on a minimum size criterion, can lead to a large potential bias at the ends of, even long subfossil, chronologies. Again we use measurement data provided by the ADVANCE-10K project (Eronen et al. 2002; Grudd et al. 2002), this time including all subfossil (from lakes and dry land) and modern core data for the last 2,000 years. These (more than 1,000) sample series were combined to produce an RCS chronology (based on a single RCS curve) shown as the solid black line in Figure 5.8a, with the temporal distribution of the sample series shown by gray shading. The data were sub-sampled to simulate eight hypothetical samplings during the last 2,000 years, separated by 200-year intervals, the most recent of which was in the year 1980. Only trees that would have been alive and that had achieved a minimum diameter of 14 cm are included in each subsample. The subsamples form a large proportion (43%) of all rings. This is a realistic simulation of common dendroclimatic sampling strategies.
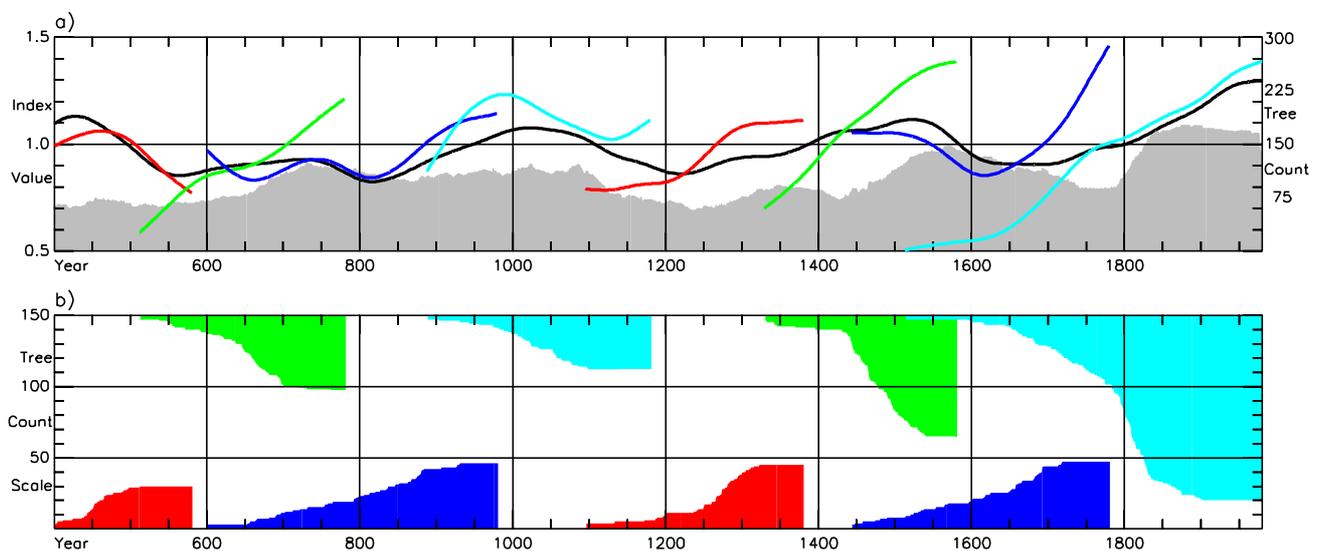
Figure 5.8. Based on 1,024 trees from AD portions of the Torneträsk and Finnish Lapland chronologies. (a) The simple regional curve standardization (RCS) chronology (black line) and associated tree counts (gray shading), truncated before AD 400. Simulated 'modern sample type' chronologies were created by averaging eight selected groups of tree indices (all produced by using the same single RCS curve and only where sample counts exceed 2). Each sub-chronology is made up of samples that would have been collected by using modern sampling practice with selections made on a series of specific dates (the first is AD 580 and subsequent selections are made every 200 years until 1980) and only including trees alive and with a diameter greater that 14 cm on the sampling date. (b) Shaded areas showing sample counts by year for each simulated chronology, plotted alternatively from the bottom and top of the figure for clarity. Approximately 43% of the total ring measurements are included in the 'selected' samples.

The temporal distribution of each 'sampled' group of trees is shown in Figure 5.8b. The eight individual sub-chronologies, each produced as the average of the index series generated in the production of the overall mean RCS chronology, are shown superimposed on the RCS chronology produced from all 1024 series. The sub-chronologies generally underestimate the mean chronology in their early years (mainly composed of older and generally slower-growing trees) and overestimate

the overall chronology in their later years (when the younger, more vigorous trees dominate the sample). This result demonstrates that sampling bias, when allied with the growth rate/longevity phenomenon, imparts negative bias in the start of a chronology and positive bias in the recent period. The systematic continuous overlaps between slower- and faster-grown trees in this example compensate throughout the chronology for these biases. That is, of course, except for the early section and, most noticeably, in the most recent 100 years of the overall chronology, which appears to follow what is likely to be a biased trajectory due to an absence of small indices from young, slow-growing trees that would have gone on to become the early sections of old trees.

5.5   Particular problems associated with the application of RCS to modern (i.e., living-tree) sample data

In practice, the underlying assumption of RCS, that the averaging of measurement series aligned by ring age and subsequent smoothing of the resulting mean curve will remove all the climate-related variance, may not always be valid. This assumption cannot be true when all samples span the full length of the chronology. In such a case, the overall climate signal will be contained within the RCS curve and will be completely removed by standardization. In a modern chronology where trees are of unequal length, the average overall slope of the chronology is contained in the RCS curve and is thus removed from every tree in the final chronology. In a long (i.e., partly subfossil) chronology, with long-timescale variation maintained in the means of each index series, this is an 'end effect.' However, where the chronology comprises one set of currently coexisting trees, as in many modern samples, the overall slope of the chronology representing the external (i.e., climate control of tree growth) will be removed. Had the chronology of Figure 5.6 had an overall downward slope, the resultant chronology would still display an upward slope (due to modern-sample bias) because the downward slope of the chronology would be removed by RCS.

Even where an uneven-aged sample of trees covers a wide time span, a localized coincidence in the temporal spans of many samples at roughly the same stage in their life span will locally bias the RCS curve. This bias is more likely near the 'old-age' section of the RCS curve, where typical low replication of very old trees leads to greater uncertainty in the RCS curve. This bias is potentially large for modern chronologies and seriously limits the application of RCS where trees come from the same time period (Briffa et al. 1996).

In a typical 'modern' dendroclimatic sample collection, the earliest measurements will come from the oldest trees cored, which tend to be slow growing. Faster-growing trees that may have been contemporaneous with the old trees in the early years will likely not have survived long enough to be included in the modern sample. Similarly, the most recent section of the chronology produced from these sampled trees would not contain data from young, slow-growing trees because these trees would not be of sufficient diameter to be considered suitable for coring. Any relatively young trees sampled would likely have to have been vigorous and growing quickly enough to allow them to attain a reasonable size in a short time. This leads to a situation where a 'modern sample' may exclude the fastest-growing trees of the earliest period and also exclude the slowest-growing trees of the most recent period. Such a sample of uneven-aged trees will be less susceptible to trend-in-signal bias, but still prone to contemporaneous-growth-rate bias, with smaller indices at the start of the chronology and larger ones at the end, imparting a positive bias on the overall chronology slope.

Figure 5.9 illustrates the use of RCS on a 'modern' chronology and the way in which a recent (ca. 1920) increase in the radial increments can influence the shape of the RCS curve. This set of 100

measurement series (each an average of data from multiple cores) from Luosto, north Finland (Melvin 2004, Section 3.2), has a wide age range. Pith-offset estimates are available for all of these data. First, an RCS curve and corresponding chronology were produced from them (thin lines in Figs. 5.9a, b). The signal-free method (see Appendix) was used to create an unbiased (signal-free) RCS curve and corresponding chronology (thick lines in Figs. 5.9a, b). The removal of the common signal from the measurements changes the shape of the RCS curve, removing the influence of the post-1920 growth increase from recent data (see values for ages 200–240 and 340 onwards in Fig. 5.9a) and produces a relative increase in the expectation of early growth (up to age 120), and a smoother, less noisy RCS curve. The resultant chronology will still suffer from bias (see sections 5.4.1–3), and the overall chronology slope is to some extent 'arbitrary' as described above. However, provided there is a wide distribution of tree ages, following the signal-free approach can mitigate the localized bias imparted by climate in the RCS curve without the need for large numbers of earlier subfossil tree data to 'average' away any modern climate signal.

Even the application of the signal-free technique is not able to mitigate the loss of the overall slope of the chronology, and a 'modern' chronology must therefore be considered as having a largely 'arbitrary' slope.
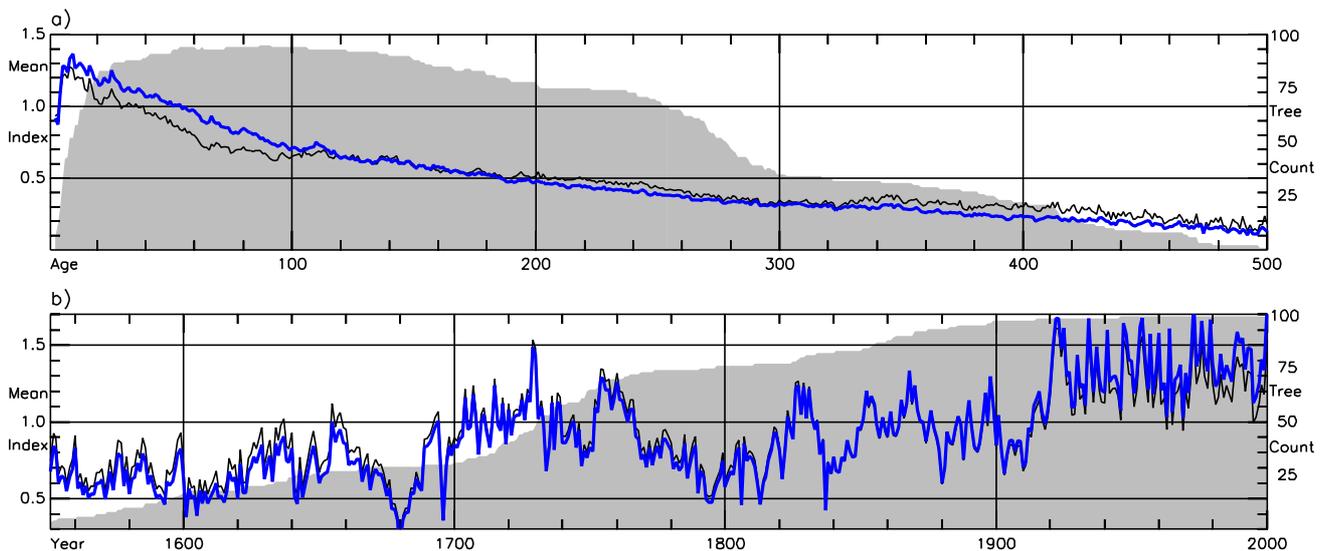
Figure 5.9. An illustration of the use of regional curve standardization (RCS) on a 'modern' chronology and the influence on the shape of the RCS curve exerted by a recent (presumably warming related) growth rate increase. The 100 mean-tree series from Luosto, north Finland (Melvin 2004), which have a wide age range and include pith-offset estimates but, after 1920, also show a large growth increase are used here: (a) a simple RCS curve (thin line) and the 'signal-free' RCS curve (thick line) and (b) the corresponding simple RCS chronology (thin line) and 'signal-free' RCS chronology (thick line). Gray shaded areas show tree counts.

5.6   Examples of issues that arise in various applications of RCS

In this section, we discuss several examples of previous work, chosen here to illustrate 'potential' bias problems that are suggested by the way in which previous authors have chosen to implement, or could be interpreted as having implemented, first, simple RCS and then variations of the simple

RCS. The three examples are based on work by Briffa et al. (1992), Esper et al. (2002), and Helama et al. (2005a, b).

5.6.1 Inappropriate RCS definition

Briffa et al. (1992) constructed separate RCS curves for ring-width (TRW) and maximum-latewood-density (MXD) data aquired from temporally overlapping subfossil and living-tree pine samples from north Sweden. The chronologies spanned the 1,480-year period from AD 501 to 1980. The ring-width RCS curve was built from 425 samples, while the density data comprised measurements made on a subsample of 65 of these trees. Though both the ring-width and density chronologies spanned more than 1,400 years, the greater replication of the data in the ring-width curve was considered more likely to have produced an 'unbiased' RCS curve (i.e., one that is not influenced by residual climate variance in the mean of the measurement data for any specific tree age). A curvilinear (negative exponential) curve was fitted to the ring width RCS curve, but a straight line was fitted to the density RCS curve (following Bräker 1981). The resulting ring-width and MXD RCS chronologies were found to diverge noticeably from each other after about 1800, with the density chronology exhibiting progressively lower index values. Briffa et al. (1992) 'corrected' this apparent anomaly by fitting a line through the residuals of actual minus estimated ring widths, derived from a regression using the density data over the period 501–1750 as the predictor variable, and then removing the recent apparent decline in the density chronology by adding the fitted straight line values (with the sign reversed) to the chronology data for 1750–1980. This 'correction' has been termed the 'Briffa bodge' (Stahle, personal communication)! In Figures 5.10 and 5.11, we show how this comparative anomaly in the density compared to the ring-width chronology arose, at least in part, because of an inappropriate representation of the density RCS curve. We use the same density data as used by Briffa et al. (1992) but use a subset of 207 ring-width measurement series from the original 425 series that were subsequently updated by Grudd et al. (2002). We have chosen to use this smaller set of measurement data because estimates of the pith offsets for these samples are now available (Kershaw 2007).

The new RCS curve (based on the smaller subset of measurements) for the ring-width data without pith-offset values (Fig. 5.10a) is effectively identical to that used in Briffa et al. (1992). With pith-offset values included, the RCS curve has a slightly higher juvenile growth-rate but tends to the same expected growth for old trees: the resulting RCS chronology (Fig. 5.11a) is not substantially different from that shown in Briffa et al. (1992), except that the 10-year-smoothed ring-width chronology is very slightly lower than that without pith estimates during the most recent 50 years. Figure 5.10d shows how the original linear RCS curve for the density data (dashed line) was not a good fit to the measured data, systematically underestimating the juvenile values and overestimating the measured data for tree ages between 250 and 500. This situation arose because the linear fit was influenced by high-density values measured in relatively old-age trees, many of which experienced the relative warmth of the twentieth century in parallel in their later years. In other words, the climate signal (as represented in the final years of the chronology) was not averaged out in the later (oldest) section of the RCS curve. A more appropriate, unbiased RCS curve is derived (the thick line of Fig. 5.10d) by using a 'signal-free' approach where the chronology variance (i.e., the best estimate of the growth-forcing signal) is iteratively removed from the measurement series so that the resulting age-aligned averaged measurements contain substantially little or no variance associated with the common forcing (see Appendix, and Melvin and Briffa 2008).
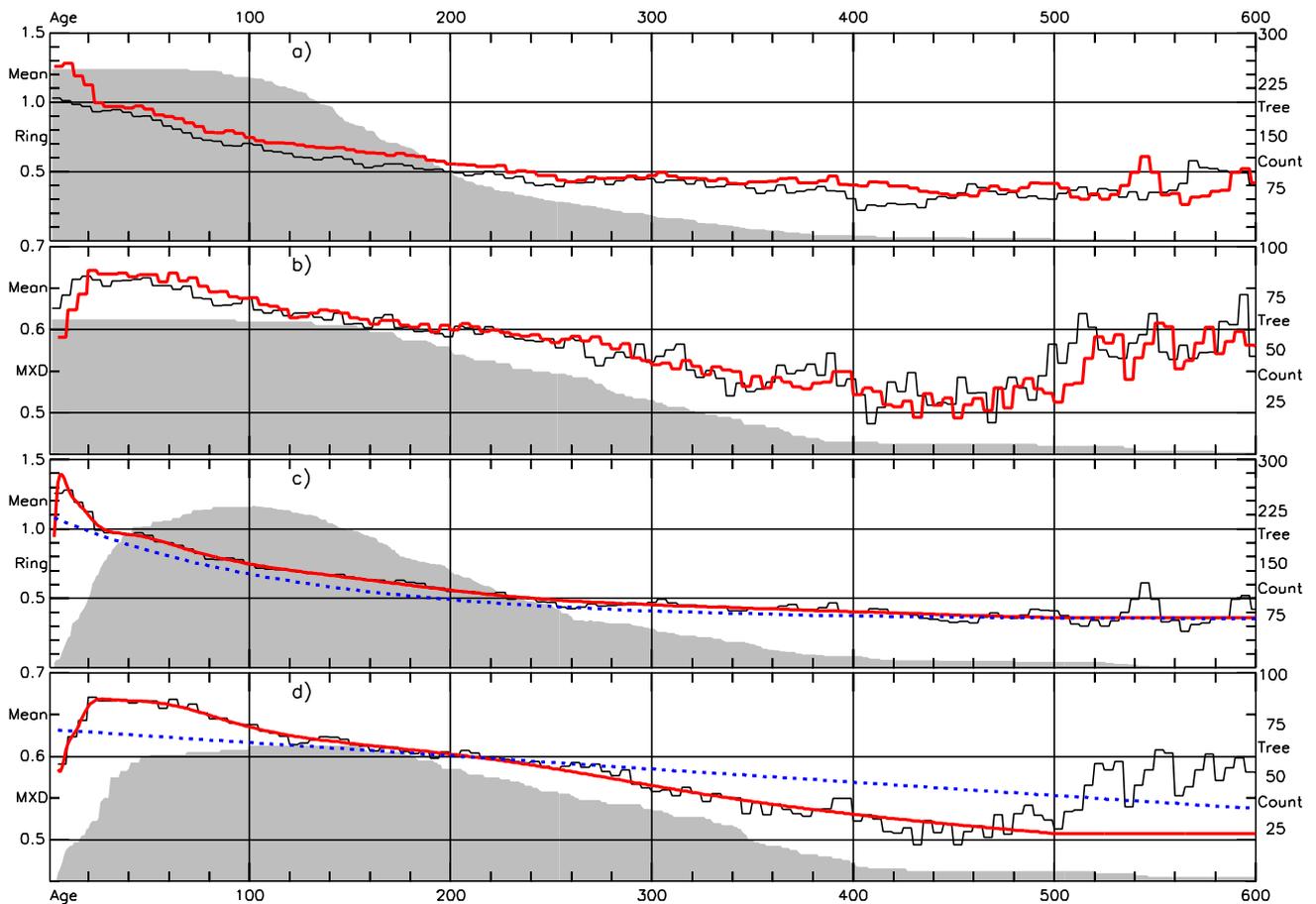
Figure 5.10. Using the 207 ring width series (TRW) with pith-offset estimates (Kershaw 2007) from the AD portion of the Torneträsk chronology (Grudd 2002) and 65 maximum latewood density series (MXD) from Torneträsk (Briffa et al. 1992b): (a) curves of 5-year means of average TRW by ring age created without using pith-offset estimates (thin line) and using pith-offset estimates (thick line); (b) as (a) but using MXD; (c) 5-year means of TRW by ring age created by using pith-offset estimates (thin line), modified negative exponential curve fitted to the ring width means created without using pith-offset estimates (dashed line) and age-related spline (thick line), fitted to the first 500 years of ring width means and then linearly extended, created by using pith-offset estimates; (d) as (c) but using MXD. Gray shading shows ring counts by age without pith-offset estimates (a and b) and with pith-offset estimates (c and d).

The density chronology produced by using the new 'unbiased' RCS curve displays potentially higher values after about 1800, and much of the comparative recent decline in the density compared to ring width chronology is removed (Fig. 5.11d). The same correction could have been achieved in this case by excluding the longest-lived tree density samples or by fitting the RCS curve only on the data extracted from tree rings up to 500 years old and extrapolating the RCS curve to give RCS values for older trees. The relevant conclusion, however, is that it is important to use a nonbiased representation of the RCS curve. Where replication is low or when there are few samples representing the expected RCS values for old trees, and especially when the oldest rings are all from trees sampled in the same period (e.g., three of the four oldest trees in the Torneträsk MXD chronology were sampled in 1982), it is particularly necessary to guard against signal bias influencing the overall shape of the RCS curve.
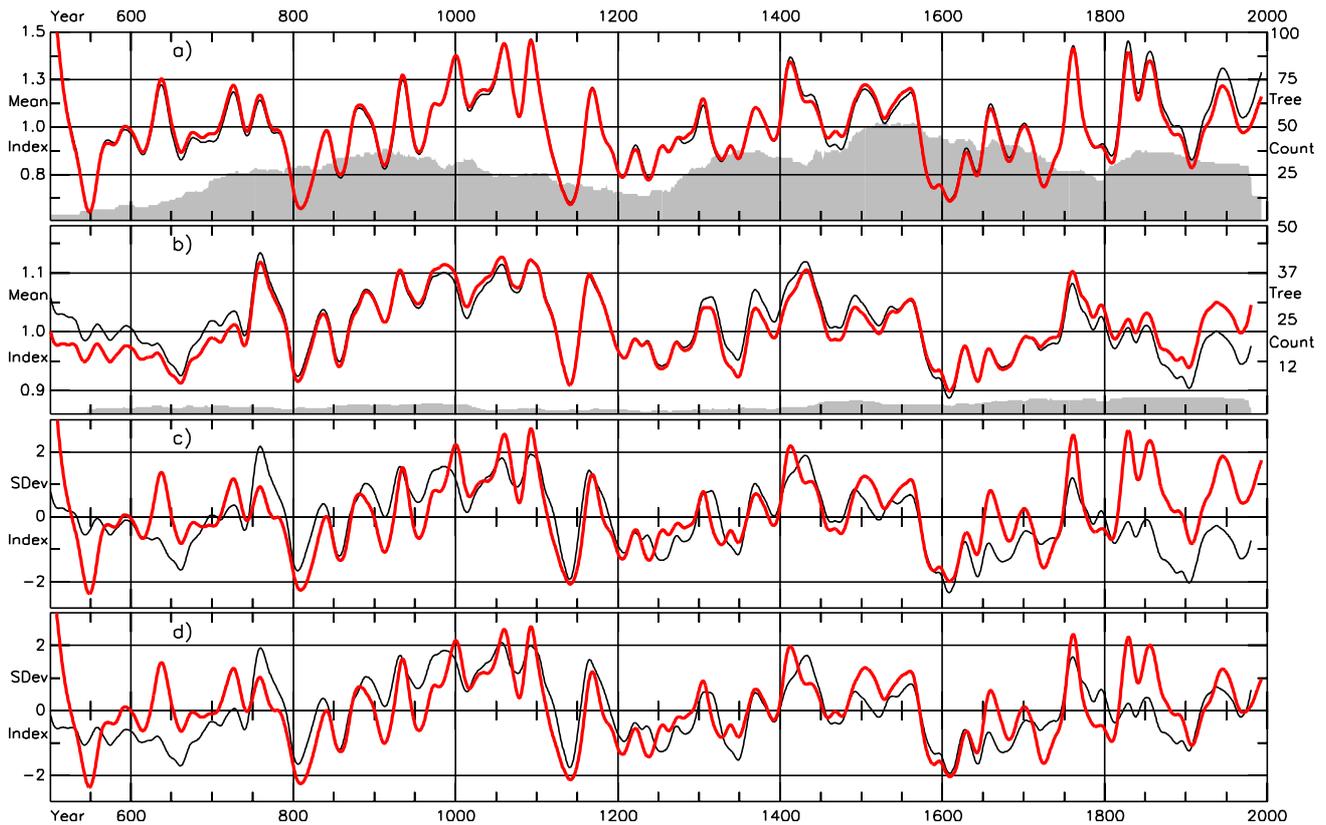
Figure 5.11. Chronologies generated by using the measurement data and regional curve standardization (RCS) curves shown in Figure 5.10: (a) ring width series (TRW) chronologies created without using pith-offset estimates and a negative-exponential RCS curve (thin linek), and with pith-offset estimates and using age-related spline smoothed RCS curve (thick line); (b) maximum latewood density series (MXD) chronologies created without using pith-offset estimates and a linear RCS curve (thin line) and with pith-offset estimates and an age-related spline smoothed RCS curve (thick line); (c) chronologies created without using pith-offset estimates, and using a negative-exponential RCS curve for TRW (thick line) and a linear RCS curve applied to MXD (thin line); (d) chronologies created by using age-related spline smoothed RCS curves and pith-offset estimates for TRW (thick line) and MXD (thin line).

5.6.2 Application of RCS across wide species and climate ranges

In their study of ring-width changes viewed over a large area of the Northern Hemisphere, Esper et al. (2002) (see also Cook et al. 2004; Frank et al. 2007) took data from 14 different locations, from various tree species, and standardized them using one of two RCS curves constructed from a subdivision of all of the measurement series. One group of measurement data displayed the familiar negative exponential pattern of declining ring width with increasing age, while the other showed a 'weakly linear' declining trend. Two RCS curves were used because it was clear that linearly declining ring growth was not well suited to scaling by the curvilinear function and vice versa. However, by incorporating data from very different species and locations in each of the linear and nonlinear RCS curves, each is unavoidably associated with wide confidence intervals. The measurements for trees at a particular site location may be systematically over- or underestimated by the use of a multisite RCS curve.

This is an extreme case of the differing-contemporaneous-growth-rate bias discussed in Section 5.4.2. The expression of this bias in the Esper et al. (2002) context is illustrated in Figure 5.12. This figure shows the local site chronologies for 5 of the 14 sites used by Esper et al.(2002), selected here to show how the use of multi-site RCS curves, whether linear or nonlinear in shape, can bias the mean of the local indices with respect to the mean indices that would have been produced by using an RCS curve derived from, and applied to, the measurement data only for the particular site. At some sites (e.g., Upperwright and Torneträsk), the bias is generally positive, while at others (e.g., Camphill) it is negative. At some sites, the mean bias is large compared to the temporal variance of the chronology (e.g., Tirol). If the regional chronologies, based on multisite-mean RCS, are simply averaged (as is implied in Esper et al. 2002), medium-frequency biases could arise in the final chronology as specific site data contained within it vary through time. In fact (though it is not apparent in Esper et al. 2002), the individual site chronologies were actually normalized prior to averaging (Ed Cook, personal communication) so that their overall means are set to a value of 1.0. This operation will mitigate much of the potential bias and effectively produce site chronologies similar to those that would be produced by using RCS applied at the site level, though medium-frequency bias will still arise where the slope of the local and multisite RCS curves differ (e.g., for Upperwright , Camphill, and Gotland; shown in Fig. 5.12).
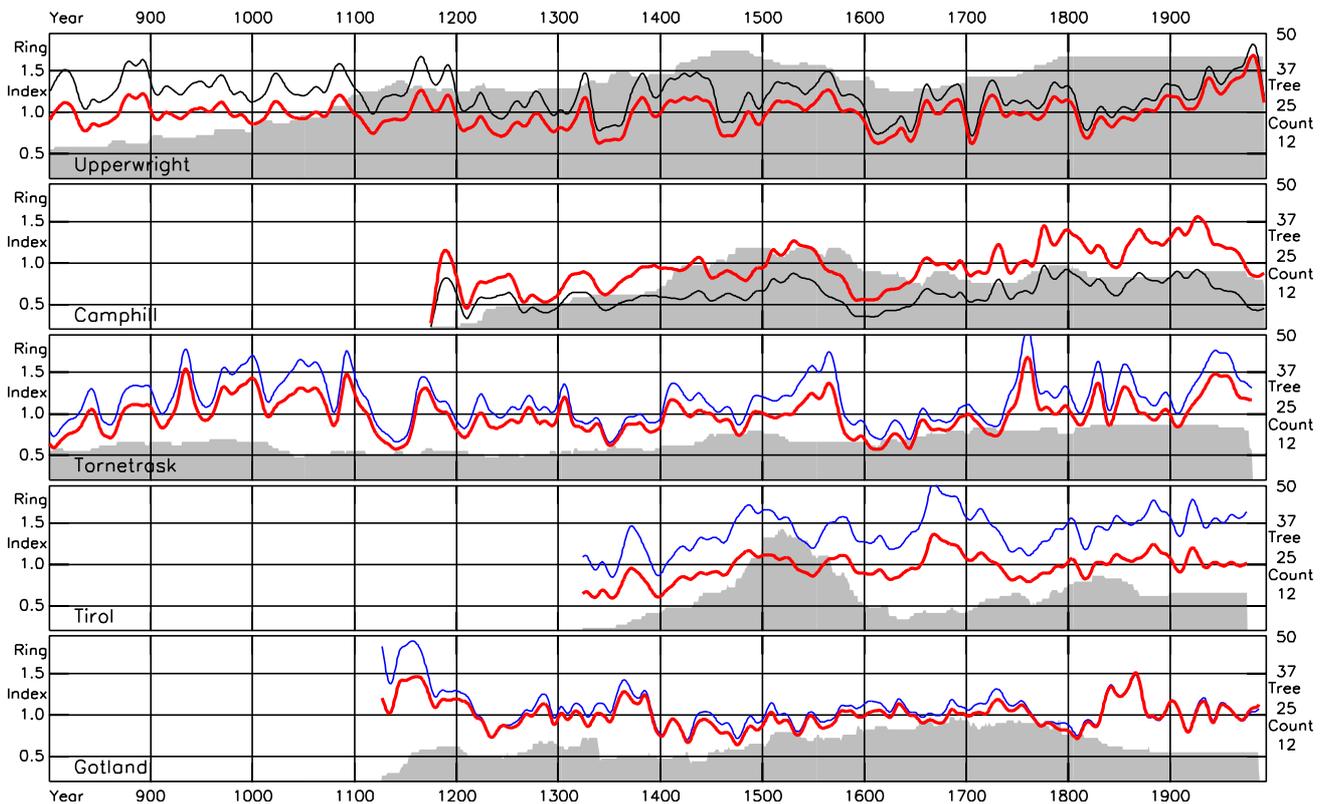
Figure 5.12. A comparison of regional curve standardized (RCS) chronologies at various sites from among those used in Esper et al. (2002). The alternative chronologies shown for each of the selected sites illustrated here were produced using different RCS curves: either that used by Esper et al. based on multi-site data (linear model for Upperwright (upper line) and Camphill (lower line) or non-linear model for Tornetrask (upper line), Tirol (upper line) and Gotland (upper line)) or a single RCS curve (thick line) based only on the data available for that site. The difference between the two curves at

each site represents a potential local bias when all chronologies are averaged to form a single 'Northern Hemisphere' series. In Esper et al. (2002) this bias was largely mitigated because each site chronology was normalized prior to averaging. For clarity all chronologies are shown as 20-year smoothed series. Sample counts are shown by gray shading.

Figure 5.13 indicates the changing effective net bias that would be associated with the application of either the mean linear form or curvilinear RCS curves to the site measurement data had the data not been normalized prior to averaging. These biases are simply the sum over all sites of the mean differences between a chronology produced by using one of the multisite RCS curves and a chronology produced by using an RCS curve applied only at a site level. (With the exception of the Mongolia data which were not available for analysis). Normalization of the individual site series largely removes this potential bias, leaving only the time-dependent changes in average site-latitude weighting applied by Esper et al. (2002) according to the site locations (presumably following the weighting normally applied in regional averaging of gridded temperature records to take account of the change of area of grid boxes with latitude when the grid is defined according to fixed latitude and longitude spacings).
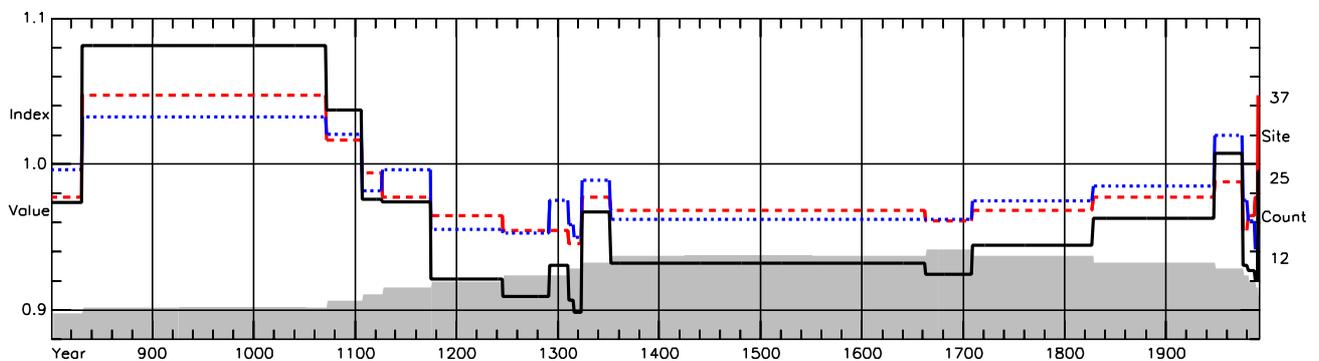
Figure 5.13. A simplified illustration of the time dependence of separate potential biases in the grand average of all local regional curve standardized (RCS) chronologies produced in Esper et al. (2002). The dotted line represents the sum, across all sites (except Mongolia, see text) of the local difference in the means of alternative chronologies, produced either with a hemispheric-data-based RCS or a local-data-based RCS curve. The mean of all individual site chronology weightings, according to site latitude (see Esper et al. 2002), is shown as a dashed line. The product of these two potential biases is shown in black. Site counts over time are shown by grey shading.

5.6.3   Adaption of RCS to account for non-climate bias

In their study of northern Finnish tree growth and climate variability during more than 7,000 years, Helama et al. (2005a,b) propose a modification of simple RCS, to take account of the changing density of forest cover, and hence competitional interactions among trees that they presume are sufficiently strong to alter the shape of the appropriate RCS curve through time. The progress of ring width decay for open-grown and close-packed trees will result in differences in the shape of RCS curves and could lead to bias in RCS chronologies, but can be evaluated only over a common 'climate' period, and it is inappropriate to disregard the background changes in the underlying climate forcing of tree growth. They first construct the basis for a conventional single RCS curve by averaging all age-aligned measurement data. To this series they fit a negative exponential with an added constant term (following Fritts et al. 1969) of the form

$$y = a * e^{-bx} + c \tag{1}$$

where the constant (a) defines the expected magnitude of the juvenile growth phase of ring growth (referred to by Helama et al. 2005a,b as the 'juvenile growth maximum'); the constant (c) defines an assumed constant growth rate of old-age trees; and constant (b) describes the rate of diminution of ring width with age (referred to by Helama et al. 2005a,b as the 'growth trend concavity').

In what they term 'environmental curve standardization (ECS), Helama et al. (2005b) do not apply this single fitted function (Eq. 1) to all of their measurement data. Instead, they perform time-dependent standardization by generating a series of RCS curves, each based on data from a 750-year time slice, overlapping each of its neighbors by 250 years. Each RCS curve is applied only to the data from the central 250 years of its corresponding time window. In this way, each 250-year non-overlapping period of the chronology is based on standardization with a different RCS curve. However, within each 250-year standardization application, only the RCS concavity (parameter b) is varied; the (a) and (c) parameters are maintained at the values calculated for the single, original overall period RCS curve.

They find a relationship between the number of tree samples (interpreted as spatial tree density) and the concavity (b) parameter (reported as 0.683, Helama et al. 2005b, Fig. 2d, and 0.73, Helama et al. 2005a, Fig. 5). The lack of any significant association between tree density and juvenile growth maximum (a) in these data (Helama et al. 2005b, Fig. 2c) presumably led them to conclude that concavity was independent of average tree growth rate.

In Table 5.1, we demonstrate that this conclusion is erroneous by using a subset of Finnish Lapland tree-ring measurements (Eronen et al. 2002; Helama et al. 2002) that form a major part (1,087 trees) of the Helama et al. (2005b) dataset (1,205 trees). Figure 5.14 shows these measurement data sorted, by relative growth rate, into six separate classes, each containing 180 or 181 trees. Growth rate was assessed according to the ratio of the radius of each tree divided by the radius of the single, overall-sample RCS curve at the point corresponding to the final age of that tree. In this way, the measurement series for all trees were divided into six groups ranging from fastest to slowest growth. For each group, a curve of mean ring width by age was produced and a modified negative exponential curve (Eq. 1) was fitted to each (Fig. 5.14b). The coefficients are shown in Table 5.1 (the (a), (b), and (c) columns).

The low numbers of older samples generally produce large inter-tree variance in these curves. With few trees (i.e., for tree ages above about 250 years) the measurement averages are erratic, so we have also calculated the curve fits only for sections of data representing the average of at least four trees. These alternative (truncated data) curve fits and their associated coefficients are also shown in Figure 5.14b and Table 5.1 (the [at], [bt], and [ct] columns). These results show that there is potentially large uncertainty in estimating the (b) coefficient where the RCS curve is fitted over sections of poorly replicated data. In our truncated group fits, removal of only 0.5% of the ring measurements on average alters the (b) parameter fits by up to 20% over the six groups. Helama et al. (2005b) calculated estimates of concavity for 28 time periods, but based on fewer trees than in this sample, and there is likely to be considerable uncertainty associated with them.

Table 5.1 also shows that there is a relationship between the juvenile growth maximum (a) and concavity (b) (r = –0.66, n = 6). This relationship is very clear in the truncated group data fits between (at) and (bt) (r = -0.96, n = 6). Similarly, the diminution in ring width over the first 50 years (Table 5.1, column [rwr]) is strongly correlated with both (a) and (b). Hence, regardless of the reason, fast-growing trees will display greater reduction of ring width. Helama et al. (2005b), by

varying (b) through time (where [a] and [c] are fixed) are standardizing the slower-growing trees with the 'higher growth rate' RCS curves and the faster-growing trees with 'lower growth rate' RCS curves (the curve with [a] and [c] held constant will have a higher rate of radial increase if [b] is small rather than large). The resulting mean values of the indices will be correspondingly greater for fast-growing trees and lower for slow-growing trees, in comparison to the means of indices generated by using a single fixed parameter RCS curve. The low-frequency variance in chronologies is imparted by changes in the means of index series.

Table 5.1. Parameters from modified negative exponential curves fitted to RCS curves.[a]

	a	b	c	at	bt	ct	rwr
Slowest	0.48	0.020	0.26	0.48	0.022	0.24	0.40
2nd	0.68	0.015	0.23	0.69	0.022	0.30	0.54
3rd	0.83	0.024	0.37	0.84	0.021	0.34	0.63
4th	0.95	0.014	0.29	0.95	0.019	0.37	0.75
5th	1.14	0.011	0.34	1.13	0.016	0.39	0.90
Fastest	1.41	0.011	0.36	1.36	0.013	0.47	1.18
Mean	0.92	0.016	0.31	0.91	0.019	0.35	
Mean difference				0.01	0.004	0.06	

[a] First a, b, and c are fitted to the full period of the regional curve standardization (RCS) curves, and second, at, bt, and ct are fitted to the truncated period of the RCS curves; i.e., the period with four or more series. 'rwr' is ring width reduction in the first 50 years of the truncated RCS curves. Values are shown for six growth rate classes, slowest to fastest. The means are shown and for the columns and also the mean differences between the full and truncated RCS curve parameters are shown. Growth rate is assessed as the ratio of the diameter growth of each tree to the diameter growth of the single RCS curve over the life of that tree.

Leaving aside the issue of whether a count of a relatively small number of tree samples through time is likely to be a realistic representation of between-tree competition when the sample area is very large and varies in its northern boundary by up to 80 km over past millennia, Helama et al. (2005b) are, in effect, amplifying the medium- to low-frequency variance in their ECS chronology by an amount that is directly proportional to the relative growth rate of the trees, regardless of whether there is any change in their direct competition status. This can be seen in the inverse pattern of variability through time of their concavity values, on the one hand, and in the difference in the ECS and RCS chronologies on the other (compare Figs. 4a and 4b in Helama et al. 2005b).

A positive association between changing concavity and tree-sample number during the last 7,000 years (see Fig. 4 in Helama et al. 2005a) may reflect a common response in both variables to changing temperature forcing; i.e., warmer periods resulting in faster tree growth (and greater decay rate of ring width) and increased germination and survival of pine trees. Were this to be true, even to some extent, the deliberate biasing of the RCS curve implicit in the ECS approach could be questionable. However, even in subfossil chronologies a period with poor overlap between two groups of contemporaneous trees can result in a period affected by this 'modern' sample bias. The most recent section of a long subfossil chronology is invariably made up of a 'modern sample' from

living trees, and the recent end of almost all such chronologies will suffer from modern-sample bias to some extent.
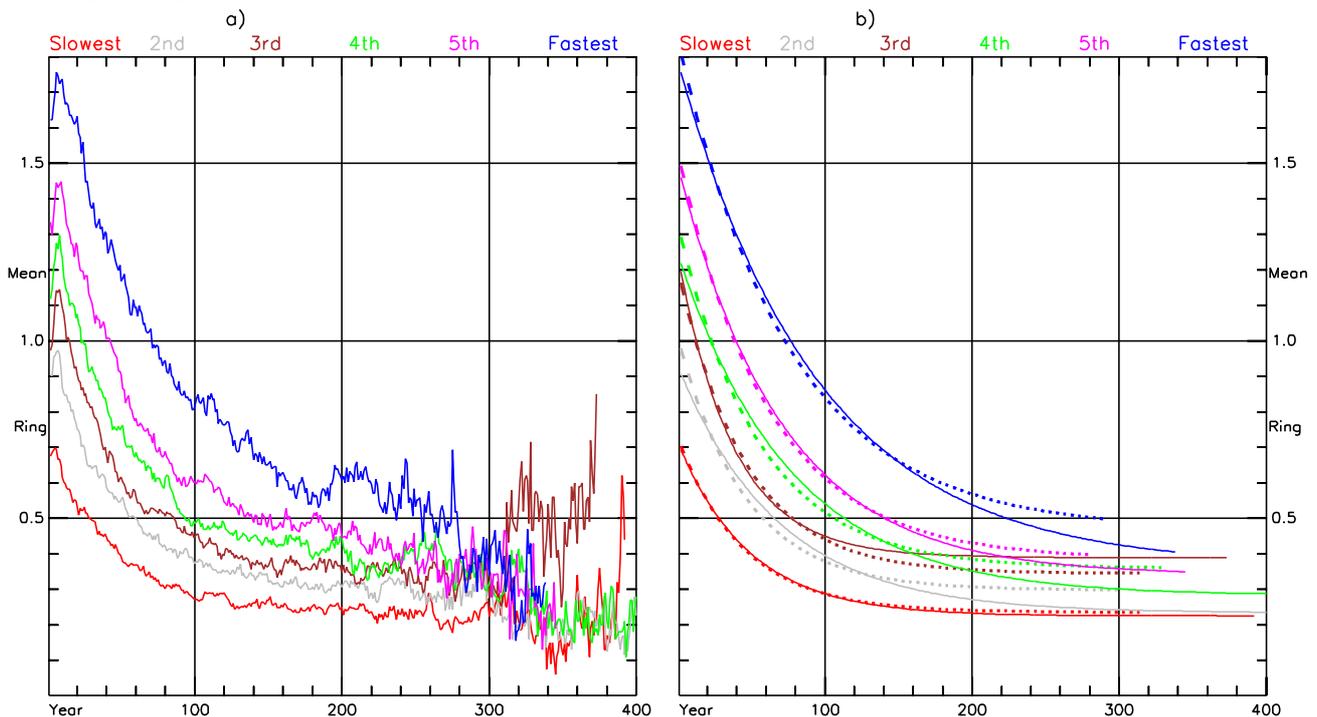
Figure 5.14: The 1,087 ring width measurement series of the Finnish Lapland chronology (Eronen 2002), without pith-offset estimates, sorted into six growth rate classes (≈180 trees in each) on the basis of the ratio of final tree radius to the radius of the single regional curve standardization (RCS) curve (at that age) created from all trees Smoothing was achieved by fitting a modified negative exponential curve to the mean series. (a) The mean ring width by age for the six growth rate classes, slowest to fastest (shaded). (b) Smoothed RCS curves for each of the six growth rate classes when fitted first to the full mean ring width by age series (continuous lines) and second when fitted to the portion of these series with sample counts of four or more trees (dotted lines).

5.7   Discussion and suggested directions for RCS development

It is the unavoidable loss of medium- and low-frequency variance, implicit in curve-fitting methods, which leads to the necessity of using RCS and the consequent requirement to recognize and overcome a number of problems associated with its specific implementation. Had the five sample series in Figure 5.2b been standardized by using curve-fitting methods, the means of each series would each be set to 1.0 and the slopes of each series would be virtually zero. All low-frequency variance would have been removed from the resulting chronology (see also Fig. 1, Briffa et al. 1996; Fig. 3, D'Arrigo et al. 2005). With curve-fitting standardization, our ability to compare the magnitude of tree growth in one decade with that in another, when they are separated by more than half the length of the constituent sample series, is potentially compromised. Hence, curve-fitting methods of tree-ring standardization are not well suited for exploring the long-term context of recent tree growth changes in response to factors such as recent temperature rises, increasing atmospheric CO_2, or other hypothesized anthropogenic influences on terrestrial ecosystems. This is the fundamental rationale for further exploring the potential, limitations, and possible improvements of RCS. A number of problems have been raised in this review, and in this final discussion we summarize several of them and point in the direction of possible solutions.

Establishing the form of the RCS curve and applying it to produce a chronology are both subject to potential biases. Bias in the form of the RCS curve arises when it erroneously tracks medium-frequency variance representing common climate signal; where the fit of expected RCS curve to the underlying age-aligned data is poor; and possibly when no allowance is made for pith offsets when aligning the underlying measurements (e.g., see Fig. 5.10d). The use of 'signal-free' methods of standardization addresses the first of these potential problems and can improve the accuracy of the RCS curve and reduce chronology error levels. These errors are generally small for long (multimillennial) chronologies but can be large for shorter chronologies. Routine implementation of signal-free methods, therefore, forms a useful extension to RCS, particularly with regard to its application in processing 'modern' chronologies. To address the second problem and to prevent loss of medium-frequency climate variance, smoothing of the RCS curve must not be too flexible, especially where sample counts are low. However, the RCS curve must be sufficiently flexible to follow the pattern of expected growth plotted against tree age accurately (Melvin et al. 2007).

The use of pith-offset estimates in generating and applying RCS curves will produce more accurate RCS curves. This increased accuracy arises because a lack of pith offsets introduces systematic bias in RCS curves, reducing the expected ring width maximum in early years of tree growth and consequently lowering the expected trend of declining growth with increasing age. Though RCS chronologies produced with and without pith offsets may be highly correlated (Esper et al. 2003; Luckman and Wilson 2005), using pith offsets may still occasionally produce more accurate chronologies (Naurzbaev et al. 2002; Melvin 2004; Büntgen et al. 2005; Esper et al. 2007), as is shown by lower chronology standard errors and a reduced frequency of local chronology bias associated with temporal concentrations of young (or old) tree samples in a chronology. The routine estimation and use of pith-offset information is, therefore, recommended.

However, other potential bias problems remain in RCS application. Any climate signal that affects the average of age-aligned sample series, e.g., the climate trend over the length of the chronology, is unavoidably removed from each series within the chronology. This trend-in-signal bias is minor for a long chronology and is manifest only at the ends, but it can be a substantial bias affecting the whole length of a short, modern chronology. Differences in the growth rates of contemporaneously growing trees, and the inadvertent acquisition of data from younger trees that are more vigorous rather than slower-growing trees in recent times, both lead to the possibility of chronologies in which more recent chronology trends may not accurately represent the influence of climate variability. This contemporaneous-growth-rate bias will cancel in all but the ends of long chronologies, but may be a serious end-effect problem manifest equally in long subfossil and modern chronologies.
Having discussed the various sources of potential bias, we now turn to the question as to relative magnitudes. No generalizations can be made, because the specific characteristics of sample data and underlying climate signal will vary in different situations. However, in an attempt to provide some illustrative indication, we offer Table 5.2. This table lists the sources and possible relative magnitudes of different biases, and makes a guess at the overall bias for a hypothetical, but not untypical, example chronology (the detailed makeup of which is described in the caption to Table 5.2) that was assumed to have been subject to a notable increase in tree growth forcing about 50–60 years ago. All the biases are manifest at the recent end and tend to reduce the expression of the expected recent growth increase over the last century of the chronology. The net biases act to produce a spurious positive trend 400 to 200 years from the end of the chronology, but the relatively large negative bias, mostly associated with non-random sampling practices, is likely to dominate in the most recent centuries.

Table 5.2. Relative sizes of individual and net bias effects.[a]

Type of RCS Bias	Effective Duration (years)	General Slope of Bias	Approximate Magnitude
Absence of pith-offset estimates	200	Negative	0.1
Trend-in-signal bias			
Solely modern chronology	200	Negative	0.1
Longer subfossil chronology	200	Negative	Negligible
Contemporaneous-growth-rate bias			
Modern sample bias	400	Positive	0.2
Dominancy of fast-growth indices	100	Negative	0.2
Net effect	400–200	Positive	0.1
	100–0	Negative	0.2

[a] These effects are implicit in the application of simple regional curve standardization (RCS) for a hypothetical chronology. These figures are 'guesstimates' of the magnitude and effective duration of RCS biases discussed in this review. These figures are expressed for a hypothetical set of data from trees with the following characteristics: the longest trees are about 400 years old; the shortest trees are around 100 years old; the chronology indices have a range from 0.5 to 1.5; and the trees experienced a 40% growth increase, which occurred around the middle of the twentieth century. These biases are manifest as 'end effects' (i.e., all terminating at the end of the chronology). All biases, with the exception of trend-in-signal bias, will apply equally to modern and sub-fossil chronologies.

The technique of aligning and averaging tree index series by ring age allows the investigation of bias. Comparison of tree indices sorted according to different criteria (e.g., by contemporaneous growth rate (Fig. 5.4b), tree age, tree diameter, latitude, altitude, aspect, or packing density) will allow the identification of potential systematic biases in RCS chronologies. The technique of 'end-aligning' (Fig. 5.7), in which both the age-related trend and the climate signal are removed, is an additional method of identifying potential bias (Section 5.4.3.2). The signal-free method is also a tool that can be used to test for residual bias in chronologies; measurement series are divided by the final chronology and the residual signal will represent bias, or the limits of the standardization method (Melvin and Briffa 2008).

The count of trees needed to produce a 'robust' chronology is often gauged by using the mean interseries correlation to calculate the expressed population signal (EPS; Wigley et al. 1984; Briffa and Jones 1990). However, estimates of EPS are strongly influenced by (biased towards) the correspondence between index series on short (primarily interannual) timescales. Experiments using ring width data from Torneträsk (Grudd et al. 2002) and Finnish Lapland (Eronen et al. 2002) have evaluated the robustness of chronology confidence in RCS. This work (Melvin 2004, Section 6.3.3) explored the influence on the standard deviations of chronologies (the average standard deviation of all yearly values) produced by varying sample counts in differently filtered tree index series. The results suggest that if a replication of 10 trees is required for a 30-year high-pass-filtered chronology to exhibit a specific mean standard deviation, a 100-year high-pass-filtered chronology would require a replication of 18 samples, while an RCS chronology would need 62 constituent samples to achieve the same standard deviation. Increasing tree counts can improve chronology confidence, but

will not remove systematic bias. Mitigating bias in RCS may improve confidence but will not remove the requirement for large sample replication.

The age band decomposition (ABD) method (Briffa et al. 2001) amounts to an alternative method of applying the RCS technique. If the mean value of each 'age band' is aligned by ring age, it will form a stepped version of the RCS curve. The ABD method therefore suffers from many of the problems of RCS, especially 'modern-sample bias,' and equal care must be taken in the use of this method and in the interpretation of the results.

Subfossil chronologies, like modern chronologies, are still susceptible to the contemporaneous-growth-rate bias. One possibility of mitigating this bias is to identify and remove the influence of fast- versus slow-grown trees, but only when they are identified in samples growing under the same climate conditions.

Some modifications of the application of RCS go some way towards obtaining these objectives, ranging from the alternative use of two sub-RCS curves (Esper et al. 2002) to the use of multiple RCS curves (Melvin 2004, Section 5.7). In the former, two different classes of RCS curve shape are identified from among those in the full dataset, and each is applied separately to the relevant group of sample series. This process removes substantial potential bias that would result from detrending series that exhibit linearly decreasing ring widths with age with an expectation of exponential decay and vice versa. However, this is an extreme example of the use of RCS, because the original sample set comprises data from various species from widely separated locations, and even the use of sub-RCS curves will not account for the large site-to-site differences in growth rates. Each sub-RCS curve will be bracketed by very wide confidence limits, leaving scope for substantial bias in the production of chronologies. Melvin (2004, Section 5.7) advocates the use of multiple RCS, in effect dividing the data on the basis of relative growth rate into a number of RCS curves, each of which is then applied to its corresponding group of measurement series to produce (where the data are continuous) multiple parallel sub-RCS chronologies. If these chronologies are then averaged together, contemporaneous-growth-rate bias will be reduced. However, this process will also remove the potential to preserve some long-timescale variance that is contained in the relative differences of the sub-RCS chronology means. There is a particular requirement for a practical way to distinguish genuine long-timescale climate signals from spurious trends that may arise in RCS, solely as a result of non-climate-related differences in the growth rates of sample trees.

Basal area increment (BAI) is a more direct measure of wood production (especially in mature trees after height increase has reduced) and BAIs are used widely in forestry. A number of researchers have used BAI chronologies as an alternative to ring widths, some employing the RCS method (e.g., Hornbeck et al. 1988; Becker 1989; Briffa 1990; Biondi et al. 1994; Rathgeber et al. 1999b). The use of BAI will likely reduce some of the problems of RCS, such as the tendency for negatively sloping indices from relatively faster-grown trees in the recent ends of chronologies and positively sloping indices from slower-growing trees, but BAI data still suffer from differing-contemporaneous-growth-rate bias and modern-sample-bias. The use of signal-free methods and the diagnostic value in examining sub-RCS curves and chronologies are equally applicable to chronologies of BAI data and, of course, to other tree-growth parameters.

5.8   Conclusions

The conceptual and practical examples of the implementation of RCS presented here are intended to demonstrate how problematic the application of a simple concept can be in practice. The recognition of the presence of bias within a chronology and the routine exploration of the magnitudes of different biases in RCS can only provide a better foundation for quantifying and expressing RCS chronology uncertainty.

The net effect of potential biases in the application of the RCS method will vary according to the specific makeup of the samples in a chronology. Much of the potential bias may average out, especially when sample replication is high, but the particular problems associated with the reliability of the start and end of chronologies may affect chronology calibration and hinder the study of recent tree-growth forcing trends. Where, by coincidence, a chronology starts around 1,000 years ago, similar problems may be associated with gauging the accurate level of tree growth at that time and perhaps, the comparative magnitude of warmth in medieval as compared to modern times.
This is not to say that biases are manifest in all RCS chronologies produced up to this time. However, it is hoped that drawing specific attention to these potential problems will stimulate a more routine approach to investigating their likely extent. This should lead to a circumspect interpretation of RCS-based climate reconstruction and provide impetus for further work aimed at improving the RCS method.

5.9   Acknowledgments

5.10   References

Badeau V, Becker M, Bert D, Dupouey J, Lebourgeois F, Picard JF (1996) Long-term growth trends of trees: ten years of dendrochronological studies in France. In: Spiecker H, Mielikainen K, Kohl M, Skovsgaard JP (eds) Growth trends in European forests. Springer, Berlin, pp 167–181.
Becker M (1989) The role of climate on present and past vitality of silver fir forests in the Vosges Mountains of northeastern France. Can J Forest Res 19:1110–1117.
Biondi F, Myers DE, Avery CC (1994) Geostatistically modeling stem size and increment in an old-growth forest. Can J Forest Res 24:1354–1368.
Bräker OU (1981) Der Alterstrend bei Jahrringdichten und Jahrringbreiten von Nadelhölzern und sein Ausgleich. Mitteilungen der Forstlichen Bundesversuchsanstalt Wien 142:75–102.
Briffa KR (1990) Increasing productivity of 'natural growth' conifers in Europe over the last century. Lundqua Report 34:64–71, Lund University, Sweden.
Briffa KR (1999) Interpreting high-resolution proxy climate data: the example of dendroclimatology. In: von Storch H (ed) Analysis of climate variability. Springer-Verlag, Heidelberg, pp 77–94.
Briffa KR, Jones PD (1990) Basic chronology statistics and assessment. In: Cook ER, Kairiukstis LA (eds) Methods of dendrochronology. Kluwer Academic, Dordrecht/Boston/London pp 137–152.
Briffa KR, Jones PD, Bartholin TS, Eckstein D, Schweingruber FH, Karlén W, Zetterberg P, Eronen M (1992) Fennoscandian summers from AD 500: temperature changes on short and long timescales. Clim Dynam 7:111–119.

Briffa KR, Jones PD, Schweingruber FH, Karlén W, Shiyatov SG (1996) Tree-ring variables as proxy-climate indicators: problems with low-frequency signals. In: Jones PD, Bradley RS, Jouzel J (eds) Climatic variations and forcing mechanisms of the last 2,000 years. Springer-Verlag, Berlin, pp 9–41.

Briffa KR, Osborn TJ, Schweingruber FH, Harris IC, Jones PD, Shiyatov SG, Vaganov EA (2001) Low-frequency temperature variations from a northern tree-ring density network. J Geophys Res-Atmos 106:2929–2941.

Büntgen U, Esper J, Frank DC, Nicolussi K, Schmidhalter M (2005) A 1,052-year tree-ring proxy for Alpine summer temperatures. Clim Dynam 25:141–153.

Cook ER (1985) A time-series analysis approach to tree-ring standardization. Ph.D dissertation, The University of Arizona, Tucson.

Cook ER, Briffa KR, Meko DM, Graybill DA, Funkhouser G (1995) The segment length curse in long tree-ring chronology development for paleoclimatic studies. Holocene 5:229–237.

Cook ER, Buckley BM, D'Arrigo RD, Peterson MJ (2000) Warm-season temperatures since 1600 BC reconstructed from Tasmanian tree rings and their relationship to large-scale sea surface temperature anomalies. Clim Dyn 16:79–91.

Cook ER, Esper J, D'Arrigo RD (2004) Extratropical Northern Hemisphere land temperature variability over the past 1,000 years. Quaternary Sci Rev 23:2063–2074.

D'Arrigo R, Mashig E, Frank D, Wilson R, Jacoby G (2005) Temperature variability over the past millennium inferred from northwestern Alaska tree rings. Clim Dyn 24:227–236.

Dewar RC (1993) A mechanistic analysis of self-thinning in terms of the carbon balance of trees. Ann Bot 71:147–159.

Dupouey J, Denis J, Becker M (1992) A new method of standardization for examining long-term trends in tree-ring chronologies. Lundqua Report 34:85–88, Lund University, Sweden.

Erlandsson S (1936) Dendrochronological studies. Geochronology Institute Report 23, University of Upsala, 1–119.

Eronen M, Zetterberg P, Briffa KR, Lindholm M, Merilainen J, Timonen M (2002) The supra-long Scots pine tree-ring record for Finnish Lapland: Part 1, chronology construction and initial inferences. Holocene 12:673–680.

Esper J, Cook ER, Schweingruber FH (2002) Low-frequency signals in long tree-ring chronologies for reconstructing past temperature variability. Science 295:2250–2253.

Esper J, Cook ER, Krusic PJ, Schweingruber FH (2003) Tests of the RCS method for preserving low-frequency variability in long tree-ring chronologies. Tree-Ring Res 59:81–98.

Esper J, Frank D, Büntgen U, Verstege A, Luterbacher J, Xoplaki, E (2007) Long-term drought severity variations in Morocco. Geophys Res Lett 34, L17702, doi:10.1029/2007GL030844.

Frank D, Esper J, Cook ER (2007) Adjustment for proxy number and coherence in a large-scale temperature reconstruction. Geophys Res Lett 34, L16709, doi:10.1029/2007GL030571

Fritts HC (1976) The statistics of ring width and climatic data. Tree Rings and Climate. Academic, London, pp 246–311.

Fritts HC, Guiot J (1990) Methods of calibration, verification, and reconstruction. In: Cook ER, Kairiukstis LA (eds) Methods of dendrochronology. Kluwer Academic, Dordrecht, pp 163–217.

Fritts HC, Mosimann JE, Bottorff CP (1969) A revised computer program for standardizing tree-ring series. Tree-Ring B 29:15–20.

Grudd H, Briffa KR, Karlén W, Bartholin TS, Jones PD, Kromer B (2002) A 7,400-year tree-ring chronology in northern Swedish Lapland: natural climatic variability expressed on annual to millennial timescales. Holocene 12:657–665.

Helama S, Lindholm M, Timonen M, Meriläinen J, Eronen M (2002) The supra-long Scots pine tree-ring record for Finnish Lapland: Part 2, interannual to centennial variability in summer temperatures for 7,500 years. Holocene 12:681–687.

Helama S, Lindholm M, Timonen M, Eronen M (2005a). Mid- and late-Holocene tree population density changes in northern Fennoscandia derived by a new method using megafossil pines and their tree-ring series. J Quaternary Sci 20:567–575.

Helama S, Timonen M, Lindholm M, Merilainen J, Eronen M (2005b) Extracting long-period climate fluctuations from tree-ring chronologies over timescales of centuries to millennia. Int J Climatol 25:1767–1779.

Hornbeck JW, Smith RB, Federer CA (1988) Growth trends in 10 species of trees in New England, 1950–1980. Can J Forest Res 18:1337–1340.

Huntington E (1913) The secret of the big trees. Department of the Interior, Washington, DC.

Huntington E (1914) The climate factor as illustrated in arid America. Pub. No. 192, Carnegie Institute, Washington. DC.

Kershaw ZL (2007). The Torneträsk tree-ring chronology: exploring the potential for biased climate reconstructions in recent millennia. Unpublished BSc thesis, University of East Anglia, UK.

Linderholm HW, Gunnarson BE (2005) Summer temperature variability in central Scandinavia during the last 3,600 years. Geogr Ann A 87A:231–241.

Luckman BH, Wilson RJS (2005) Summer temperatures in the Canadian Rockies during the last millennium: a revised record. Clim Dynam 24:131–144.

Melvin TM (2004) Historical growth rates and changing climatic sensitivity of boreal conifers. Thesis. University of East Anglia, Norwich, UK. http://www.cru.uea.ac.uk/cru/pubs/thesis/2004-melvin/.

Melvin TM, Briffa KR (2008) A "signal-free" approach to dendroclimatic standardisation. Dendrochronologia 26:71-86

Melvin TM, Briffa KR, Nicolussi K, Grabner M (2007) Time-varying-response smoothing. Dendrochronologia 25:65–69.

Mitchell VL (1967) An investigation of certain aspects of tree growth rates in relation to climate in the central Canadian boreal forest. Technical report 33, University of Wisconsin, Department of Meteorology.

Naurzbaev MM, Vaganov EA, Sidorova OV, Schweingruber FH (2002) Summer temperatures in eastern Taimyr inferred from a 2,427-year late-Holocene tree-ring chronology and earlier floating series. Holocene 12:727–736.

Naurzbaev MM, Hughes MK, Vaganov EA (2004) Tree-ring growth curves as sources of climatic information. Quaternary Res 62:126–133.

Nicolussi K, Bortenschlager S, Körner C (1995) Increase in tree-ring width in sub-Alpine Pinus cembra from the central Alps that may be CO_2 related. Trees-Struct Funct 9:181–189.

Rathgeber C, Guiot J, Roche P, Tessier L (1999a) Augmentation de productivité du chêne pubescent en région méditerranéenne française. Ann For Sci 56:211–219.

Rathgeber C, Guiot J, Roche P, Tessier L (1999b) Quercus humilis increase of productivity in the Mediterranean area. Ann For Sci 56:211–219.

Schweingruber F, Briffa KR (1996) Tree-ring density networks for climatic reconstruction. In: Jones PD, Bradley RS (eds) NATO Series, Vol I 41, Climatic variations and forcing mechanisms. Springer-Verlag, Berlin.

Wigley TML, Briffa KR, Jones PD (1984) On the average value of correlated time series with applications in dendroclimatology and hydrometeorology. J Clim Appl Meteorol 23:201–213.

Wilson RJS, Luckman BH, Esper J (2005) A 500-year dendroclimatic reconstruction of spring-summer precipitation from the lower Bavarian Forest region, Germany. Int J Climatol 25:611–630.

Appendix: Signal-free standardization

In this review, we make several references to the 'signal-free' method in tree-ring standardization (see Sections 5.4.1, 5.5, 5.6.1, and 5.7). A more detailed discussion of the topic (in the context of 'data-adaptive' standardization involving 'curve fitting' to individual measured series) can be found in Melvin and Briffa (2008). However, for the convenience of the reader, a brief description of the rationale and application of the signal-free approach is provided here.

Background and rationale

The signal-free concept stems from the observation that individual tree-ring measurement series represent a mixture of potential growth influences, among which are included first, that of climate variability through time and second, that of changing allocation processes and tree geometry that both affect the size of annual stem increments. Standardization has always aimed to remove or reduce the allocation bias; e.g., the signal of reducing ring width with age, so that the remaining variability in ring width indices over time provides a clearer representation of the influence of climate variability. Developing standardization curves from measurement series that contain the climate signal, where the standardization curve may track the climate signal, at least to some extent, will lead to the removal of some climate-related variance and so bias the resulting chronology. This bias is well known with respect to the removal of variance representing timescales longer than the typical life span of the sample trees (Cook et al. 1995). However, it can also arise where a common, externally forced growth signal influences the more localized fit of a standardization curve, resulting in the partial, or even complete, loss of a relatively short-term climate signal (in the case of more flexible standardization curves) and the distortion of medium-term climate trends in adjacent periods (where less flexible, but still 'fitted,' standardization functions are employed). The rationale behind 'signal-free' standardization is that it should be possible to produce an improved (i.e., locally unbiased) chronology if the individual measurement series could be detrended without allowing the fitting of standardization curves to be affected by the presence of climatically forced variability. One suggestion for achieving this condition is to remove the common variability (chronology signal) from all measurement series to yield less-biased detrending curves.

Implementing signal-free standardization

Melvin and Briffa (2008) describe one such approach, applied in the context of 'curve-fitting' standardization using options offered in the ARSTAN program (Cook 1985). They demonstrate how a combination of the 'segment length curse' and localized distortion of standardization curves can produce a biased ring-width chronology, apparent as a failure by the standardized chronology to express recent climatic trends. Details of their implementation of this signal-free approach, in the context of curve-fitting standardization, are given in Melvin and Briffa (2008).

When this approach is applied in the case of regional curve standardization (RCS), a first chronology is produced by division of the tree-ring measurements by the appropriate RCS curve values. Each original measurement value is then divided by the appropriate chronology value for that year to produce a first set of 'signal-free' measurements. The standardization is then repeated on these signal-free data, and a new chronology is produced from the new signal-free indices. The process is repeated until the point where the signal-free data make up a chronology that has virtually zero variance. In practice, the magnitude of residual bias (i.e., as represented by the variance of the signal-free chronology) after each iteration is 20% of its initial value. A zero-variance signal-free chronology is considered here to be one where all values are within the range 1.0 ± 0.002. This condition is achieved generally within four or five signal-free iterations. At this point, the final RCS curve is unaffected by any external growth-forcing signal and should, therefore, yield a less-biased chronology.